Dyes and Pigments 194 (2021) 109644

Contents lists available at ScienceDirect

Dyes and Pigments

journal homepage: www.elsevier.com/locate/dyepig

Red light-emitting Carborane-BODIPY dyes: Synthesis and properties of visible-light tuned fluorophores with enhanced boron content

Chiara Bellomo [a,1], Davide Zanetti [a,1], Francesca Cardano [a], Sohini Sinha [b], Mahdi Chaari [b], Andrea Fin [c], Andrea Maranzana [a], Rosario Núñez [b,**], Marco Blangetti [a,*], Cristina Prandi [a,***]

[a] Dipartimento di Chimica, Università degli Studi di Torino, via P. Giuria 7, I-10125, Torino, Italy
[b] Instituto de Ciencia de Materiales de Barcelona, ICMAB-CSIC, Campus de la UAB, 08193, Bellatera, Barcelona, Spain
[c] Dipartimento di Scienza e Tecnologia del Farmaco, Università degli Studi di Torino, via P. Giuria 9, I-10125, Torino, Italy

ARTICLE INFO

Keywords:
Carborane
BODIPY
Dyads
Photoluminescent material
Heck coupling

ABSTRACT

A small library of 2,6- and 3,5-distyrenyl-substituted carborane-BODIPY dyes was efficiently synthesized by means of a Pd-catalyzed Heck coupling reaction. Styrenyl-carborane derivatives were exploited as molecular tools to insert two carborane clusters into the fluorophore core and to extend the π-conjugation of the final molecule in a single synthetic step. The synthetic approach allows to increase the molecular diversity of this class of fluorescent dyes by the synthesis of symmetric or asymmetric units with enhanced boron content. The structural characterization and the photoluminescence (PL) properties of synthesized dyes were evaluated, and the structure/properties relationships have been investigated by theoretical calculations. The developed compounds exhibit a significant bathochromic shift compared to their parent fluorophore scaffolds, and absorption and emission patterns were practically unaffected by the different substituents (Me or Ph) on the $C_{cluster}$ atom (C_c) of the carborane cage or the cluster isomer (*ortho*- or *meta*-carborane). Remarkably, the presence of carborane units at 2,6-positions of the fluorophore produced a significant increase of the emission fluorescent quantum yields, which could be slightly tuned by changing the C_c-substituent and the carborane isomer, as well as introducing ethylene glycol groups at the *meso*-position of the BODIPY.

1. Introduction

The fascinating chemistry of polyhedral boron-carbon clusters has experienced an exponential and overwhelming growth since their discovery in the 1960s [1]. Icosahedral carborane derivatives have been the subject of an intense research owing to their unique properties such as high chemical and thermal stability [2], delocalized three-dimensional aromaticity [3], high hydrophobicity and enriched boron content [4], electron-withdrawing character [5] and high biocompatibility [6]. The remarkable physico-chemical features of carboranes and their versatility toward functionalization [7] have been widely exploited in several areas including medicine (as anticancer agents for boron neutron capture therapy (BNCT) and pharmacophores) [7b, 8], catalysis [9], optoelectronic (as non-linear optical materials and liquid crystals) [10], and nanomaterials [11]. Additionally, the development of fluorescent materials incorporating carboranes has significantly increased in the last decade [2a, 12], and their photoluminescent (PL) behavior has been deeply investigated. As a result, the carborane cage linked to certain species (e.g. small fluorophores) directly influences both the PL properties and the thermal stability of the final material [13], offering new outstanding opportunities toward the development of luminescent materials, organic field-effect transistors (OFETs) [14], phosphorescent organic light emitting diodes (PHOLEDs) [15], and biomedical tools (mainly bioimaging for diagnosis) [16]. Owing to their unique spectroscopic features BODIPY dyes (4,4-difluoro-4-bora-3a,4a-diaza-*s*-indacene) [17] represent a very interesting class of fluorophores for carborane functionalization. Moreover, the countless pre- and post-functionalization synthetic pathways of the BODIPY core allows its easy linkage to the carborane cluster using common synthetic procedures. Several carboranyl-BODIPY dyads with

* Corresponding author.
** Corresponding author.
*** Corresponding author.
E-mail addresses: rosario@icmab.es (R. Núñez), marco.blangetti@unito.it (M. Blangetti), cristina.prandi@unito.it (C. Prandi).
[1] These authors contributed equally to this work.

https://doi.org/10.1016/j.dyepig.2021.109644
Received 9 February 2021; Received in revised form 17 June 2021; Accepted 11 July 2021
Available online 14 July 2021

remarkable PL properties for luminescent devices and BNCT purposes have been thus synthesized in the last few years by means of Pd-catalyzed cross coupling reactions or alkyne insertion into decaborane [18]. In the course of our studies aimed at exploiting the photophysical properties of BODIPY dyes for biological applications [19], we recently reported the first synthesis of a small family of carborane-(aza) BODIPY dyads by means of a convergent Heck coupling approach, starting from a styrenyl-containing carborane and a brominated (aza) dipyrromethene fluorophore [20]. Although these styrenyl carborane-BODIPY derivatives preserved the photophysical features of the fluorophore, the design of new dyes with optical properties shifted toward the near-infrared region and into the therapeutic window in biological tissues still remains an urgency in view of biomedical applications of these compounds [21]. Moreover, the need to perform efficient boron rich carriers to find novel potential candidates for BNCT is still on the rise.

To this purpose, we planned to synthesize a new family of styrenyl carborane-BODIPY dyes exhibiting a whole π-conjugate system through the entire backbone of the molecule. In view of the development of bright and stable fluorophores emitting in the red spectral region, the extension of π-conjugation is essential for obtaining a bathochromic shift of both absorbance and emission maxima. The introduction of styrenyl groups on the BODIPY core at the 3,5- and 1,7-positions is one of the most efficient strategies toward a significant redshift of the spectral bands [22], while to the best of our knowledge only one example of 2, 6-distyrenyl substituted BODIPY dyes has been reported so far [23].

On the basis of these considerations and motivated by our ongoing interest in the design of new fluorescent and high boron content carborane-based scaffolds, we herein report the Pd-catalyzed synthesis of a small library of red-light emitting carborane-BODIPY dyads linked at the 2,6-positions and 3,5-positions with a π-conjugated styrene moiety spacer (Fig. 1). The rationale of this work focuses on the following key points. a) Styrenyl carborane derivatives are exploited as molecular tools to extend the π-conjugation of the final molecule and insert two boron-carbon cages into the fluorophore in a single synthetic step. This aspect is crucial in view of future developments of these dyes for bioimaging applications, since fulfils the need for new dyes absorbing in the therapeutical window. Furthermore, the presence of two carborane units linked to a BODIPY fluorophore might significantly improve the cellular uptake of the dyes, especially for *m*-carborane derivatives [18a]. b) The high chemical versatility of the BODIPY core allows to enlarge the molecular diversity of the fluorescent dyes by the synthesis of symmetric or asymmetric units, and c) the introduction of two carborane units enhances the boron content of the dyes, improving the prospective applications of carborane-BODIPY dyes as potential boron carriers for BNCT applications. To this purpose, a series of *ortho*- and *meta*- (*o*- and *m*-) substituted styrenyl-carboranes were linked to suitable BODIPY dyes halogenated at the 2,6- and 3,5-positions by means of a Heck coupling approach. The spectroscopic and photophysical properties are discussed, and theoretical investigations have been accomplished in order to clarify the structure/properties relationships of the new dyes.

2. Experimental section

2.1. Materials and methods

Unless specified, all reagents were used as received without further purifications. $[Pd_2(dba)_3]$, $[Pd(t\text{-}Bu_3P)_2]$ and Cy_2NMe were purchased from Aldrich. All reactions involving air-sensitive reagents were performed under nitrogen in oven-dried glassware using the syringe septum cap technique. Anhydrous CH_2Cl_2 was obtained by distillation over CaH_2. Anhydrous THF was obtained by distillation over $LiAlH_4$, followed by distillation over Na-benzophenone. Et_3N was distilled over CaH_2 and dry 1,4-dioxane was purchased from Merck-SigmaAldrich and used as received. Reactions were monitored using thin layer chromatography on silica gel coated aluminium plates. Chromatographic separations were performed under pressure on silica gel (40–63 μm, 230–400 mesh). R_f values refer to TLC carried out on silica gel plates with UV light (254 nm and/or 366 nm) as visualizing agent.

2.2. Instrumentation

^1H NMR (600 MHz) and $^{13}C\{^1H\}$ (150 MHz) NMR spectra were recorded in $CDCl_3$ on a Jeol ECZR600 spectrometer at RT using residual solvent peak as an internal standard. $^{11}B\{^1H\}$ (128.38 MHz) NMR spectra were recorded on a Bruker ARX 400 spectrometer in $CDCl_3$. Chemical shift values for $^{11}B\{^1H\}$ NMR spectra were referenced to external $BF_3{\cdot}OEt_2$, those for ^1H and $^{13}C\{^1H\}$ NMR were referenced to [Si

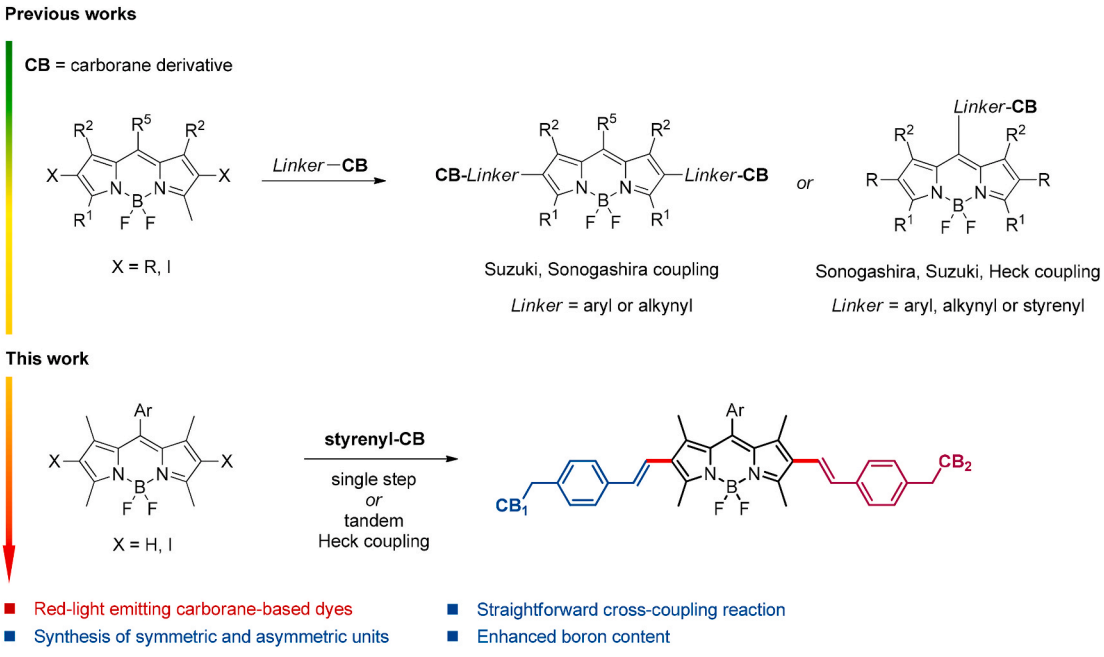

Fig. 1. Aim of the work.

$(CH_3)_4$] (TMS). Chemical shifts (δ) are given in parts per million (ppm) and coupling constants (J) in Hertz (Hz). Multiplicities are reported as follows: *s* (singlet), *d* (doublet), *t* (triplet), *q* (quartet), *m* (multiplet). Low-resolution mass spectra were recorded on a Micromass Quattro microTM API (Waters Corporation, Milford, MA, USA) or at an ionizing voltage of 70 eV on a HP 5989B mass selective detector connected to an HP 5890 GC with a methyl silicone capillary column (EI). The MS flow-injection analyses were run on a high resolving power hybrid mass spectrometer (HRMS) Orbitrap Fusion (Thermo Scientific, Rodano, Italy), equipped with an ESI ion source. The samples were analyzed in acetonitrile solution using a syringe pump at a flow rate of 5 μL/min. The tuning parameters adopted for the ESI source were: source voltage 4.0 kV. The heated capillary temperature was maintained at 275 °C. The mass accuracy of the recorded ions (vs. the calculated ones) was ±2.5 mmu (milli-mass units). Analyses were run using both full MS (150–2000 *m/z* range) and MS/MS acquisition, at 500000 resolutions (200 *m/z*).

2.3. Syntheses and characterizations

Iodinated BODIPY dyes **1a** [24], **1c** [25], **1d** [26] and styrenyl-containing carboranes [12l] ***m*-Me-CB**, ***o*-Ph-CB** and ***m*-Ph-CB** were synthesized according to the procedures reported in literature. Mono-iodinated BODIPY dye **1b** was synthesized starting from the corresponding 4-alkoxy substituted benzaldehyde (see Supporting Information for full synthetic details). Full characterization data, including copies of ^{1}H and ^{13}C NMR spectra (see Supporting Information), have been reported for the newly synthesized compounds. The syntheses of 2, 6-disubstituted styrenyl-carborane BODIPY dyes are depicted in Scheme 1 (**2**, **2a**) and Scheme 2 (**3–8**). The synthesis of 3,5-disubstituted styrenyl-carborane BODIPY dye **9** is illustrated in Scheme 3.

*General procedure (**A**) for the Heck coupling reactions.* A round-bottomed flask equipped with a condenser was charged with 3 mL of dry 1,4-dioxane, and the solvent was degassed with nitrogen for 15 min. The appropriate styrenyl-containing carborane (2.1 equiv.) and iodinated BODIPY derivatives **1a-b** or **1d** (1 equiv.) were added, followed by [$Pd_2(dba)_3$] (3 mol%), [Pd(*t*-$Bu_3P)_2$] (6 mol%) and Cy_2*N*Me (4.8 equiv.). The reaction mixture was heated at reflux overnight. After complete conversion of the starting material (as monitored by TLC analysis), the mixture was filtered over celite, washed with THF and concentrated to dryness. The crude residue was purified by flash column chromatography on silica gel.

*General procedure (**B**) for the Heck coupling reactions.* A round-bottomed flask equipped with a condenser was charged with 3 mL of dry 1,4-dioxane, and the solvent was degassed with nitrogen for 15 min. The appropriate styrenyl-containing carborane (1 equiv.) and the styrenyl-carborane BODIPY derivative **6** (1.1 equiv.) were added, followed by [$Pd_2(dba)_3$] (5 mol%), [Pd(*t*-$Bu_3P)_2$] (5 mol%) and Cy_2*N*Me (1.34 equiv.). The reaction mixture was heated at reflux overnight. After complete conversion of the starting material (as monitored by TLC analysis), the mixture was filtered over celite, washed with THF and concentrated to dryness. The crude residue was purified by flash column chromatography on silica gel.

Synthesis and characterization of compound 2. General procedure (**A**) starting from **1a** and ***m*-Me-CB**. Purification by flash column chromatography on silica gel (PE/DCM 6/4 v/v) gave **2** as a bright blue solid. (43%, R_f = 0.5 PE/DCM 6/4 v/v). ^{1}H NMR (600 MHz, $CDCl_3$): δ 7.54–7.52 (m, 3H), 7.37 (d, J = 8.2 Hz, 4H), 7.34–7.33 (m, 2H), 7.07 (d, J = 8.2 Hz, 4H), 6.87 (d, J = 16.5 Hz, 2H), 6.63 (d, J = 16.5 Hz, 2H), 3.18 (s, 4H), 2.74 (s, 6H), 1.64 (s, 6H), 1.47 (s, 6H). ^{13}C{^{1}H} NMR (150 MHz, $CDCl_3$) δ: 155.4, 141.6, 138.9, 137.1, 136.4, 135.4, 131.6, 131.0, 130.4, 129.4, 129.3, 129.0, 128.4, 128.2, 126.2, 120.0, 70.9, 42.8, 24.7, 14.2, 13.1. ^{11}B{^{1}H} NMR (128.38 MHz, $CDCl_3$) δ: 0.99 (s, 1B, BF_2) −6.17 (s, 2B), −7.88 (s, 2B), −10.50 (br s, 12B), −13.04 (s, 4B). ESI-HRMS $[M+Na]^+$: *m/z* 891.6674; $C_{43}H_{59}B_{21}F_2N_2Na^+$ requires 891.6638.

Synthesis and characterization of compound 2a. Isolated by flash column chromatography on silica gel (PE/DCM 6/4 v/v) from the crude reaction mixture giving compound **2a** (6%, R_f = 0.6 PE/DCM 6:4 v/v). ^{1}H NMR (600 MHz, $CDCl_3$): δ 7.50–7.49 (m, 3H), 7.38 (d, J = 8.2 Hz, 2H), 7.35–7.33 (m, 2H), 7.23 (d, J = 8.3 Hz, 2H), 7.07 (d, J = 8.2 Hz, 2H), 7.02 (d, J = 8.3 Hz, 2H), 6.88 (d, J = 16.5 Hz, 1H), 6.63 (d, J = 16.5, 1H), 5.84 (s, 1H), 5.10 (s, 1H), 3.18 (s, 2H), 3.16 (s, 2H), 2.73 (s, 3H), 2.37 (s, 3H), 1.64 (s, 3H), 1.63 (s, 3H), 1.48 (s, 3H), 1.22 (s, 3H). ^{13}C {^{1}H} NMR (150 MHz, $CDCl_3$): δ 155.2, 155.0, 140.7, 140.5, 139.4, 138.8, 136.7, 136.3, 135.3, 131.5, 130.8, 130.3, 130.1, 129.3, 129.2, 128.7, 128.2, 126.5, 126.2, 120.1, 117.6, 80.4, 70.8, 42.7, 42.6, 29.8, 24.6, 14.1, 13.5, 13.0, 12.9. ^{11}B{^{1}H} NMR (128.38 MHz, $CDCl_3$) δ: 1.01 (s, 1B, BF_2), −6.24 (s, 2B), −7.91 (s, 2B), −10.50 (br s, 12B), −13.04 (s, 4B). ESI-HRMS $[M+Na]^+$: *m/z* 891.6618; $C_{43}H_{59}B_{21}F_2N_2Na^+$ requires 891.6638.

Synthesis and characterization of compound 3. General procedure (**A**) starting from **1a** and ***m*-Ph-CB**. Purification by flash column

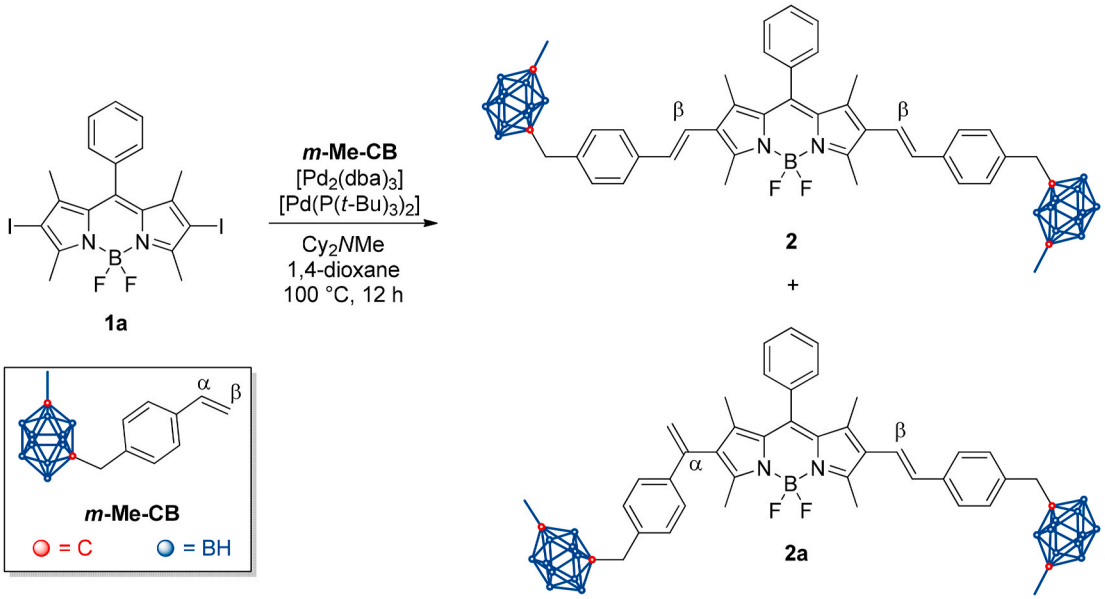

Scheme 1. Model Heck coupling reaction for the synthesis of 2,6-bis(styrenylcarborane)-BODIPY dyes.

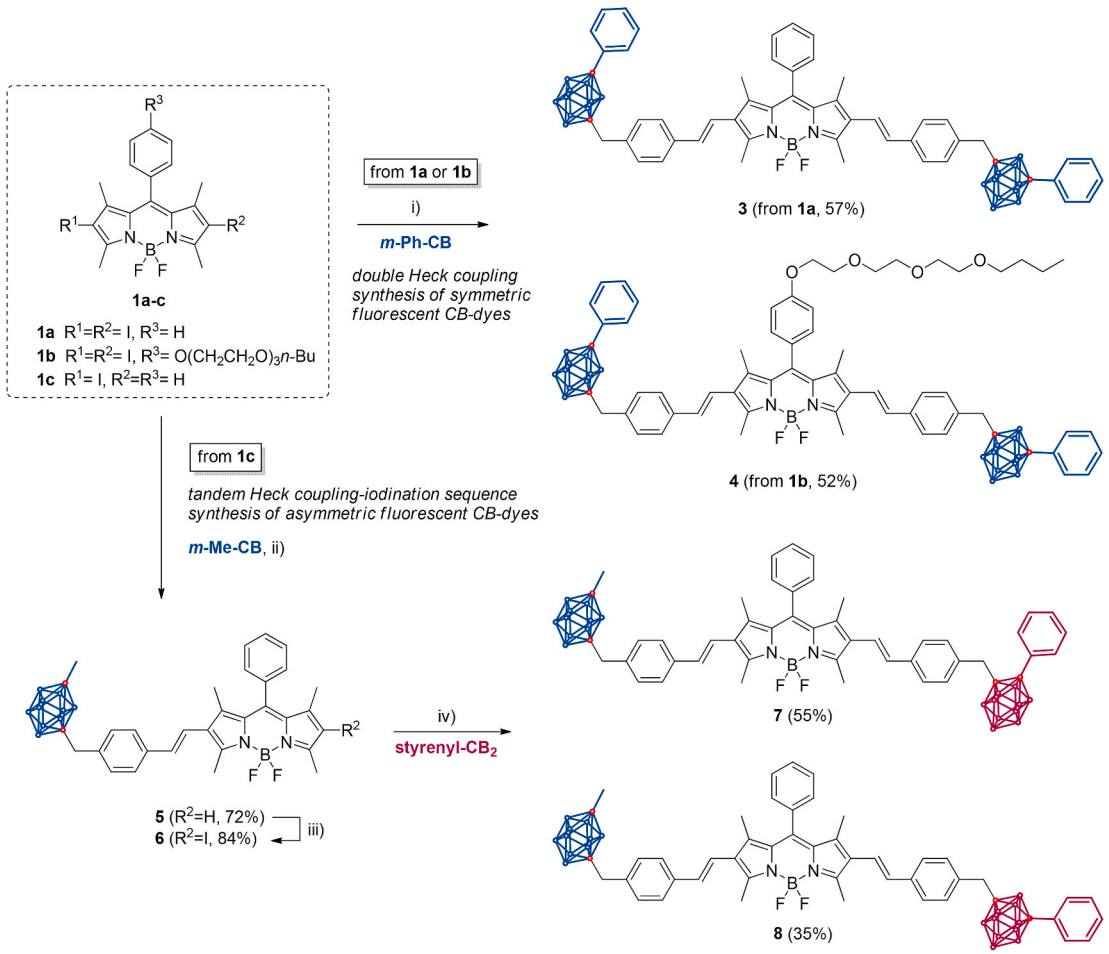

Scheme 2. Synthesis of symmetric and asymmetric carborane-BODIPY dyes **3–4** and **7–8**. Reaction conditions: i) substrate **1a-b** (1 eq.), ***m*-Ph-CB** (2 eq.), $[Pd_2(dba)_3]$ (3 mol%), $[Pd(t\text{-}Bu_3P)_2]$ (6 mol%), Cy_2NMe (5 eq.). ii) **1c** (1.1 eq.), ***m*-Me-CB** (1 eq.), $[Pd_2(dba)_3]$ (1.2 mol%), $[Pd(t\text{-}Bu_3P)_2]$ (1.6 mol%), Cy_2NMe (1.4 eq.), dry 1,4-dioxane, 100 °C, 12 h. iii) **5** (1 equiv.), *N*-iodosuccinimide (2 eq.), DCM, RT, 12 h. iv) **6** (1.1 eq.), **styrenyl-CB$_2$** (1 eq.), $[Pd_2(dba)_3]$ (5 mol%), $[Pd(t\text{-}Bu_3P)_2]$ (5 mol%), Cy_2NMe (1.4 eq.), dry 1,4-dioxane, 100 °C, 12 h.

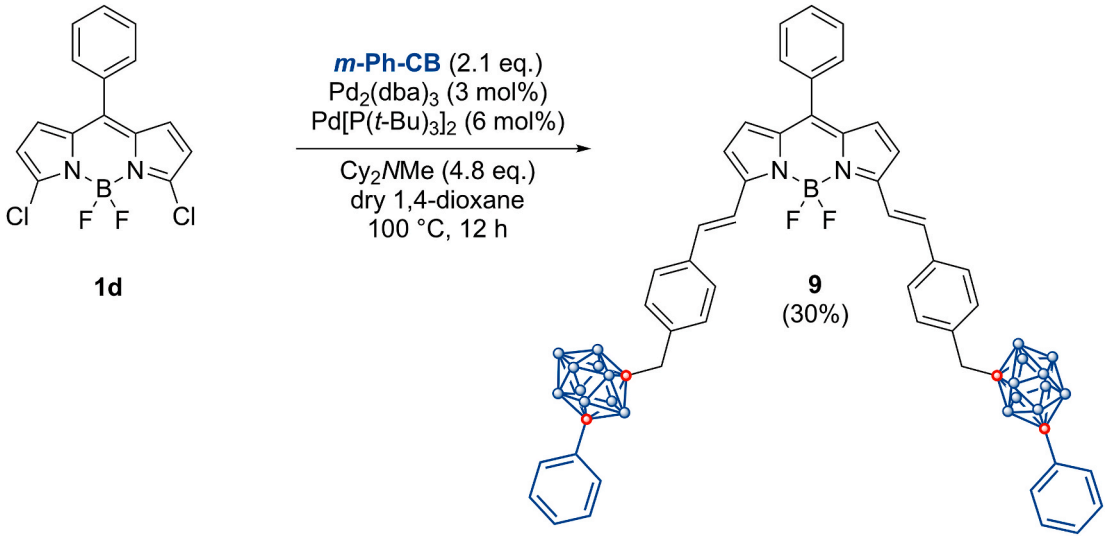

Scheme 3. Synthesis of symmetric 3,5-disubstituted BODIPY dye **9**.

chromatography on silica gel (PE/DCM 6/4 v/v) gave **3** as a bright blue solid (57%, R_f = 0.4 PE/DCM 6/4 v/v). ^{1}H NMR (600 MHz, $CDCl_3$): δ 7.49–7.40 (m, 4H), 7.33–7.24 (m, 11H), 7.15 (d, J = 7.9 Hz, 4H), 7.02 (d, J = 7.9 Hz, 4H), 6.80 (d, J = 16.5 Hz, 2H), 6.55 (d, J = 16.5 Hz, 2H), 3.18 (s, 4H), 2.66 (s, 6H), 1.40 (s, 6H). $^{13}C\{^1H\}$ NMR (150 MHz, $CDCl_3$): δ 155.3, 141.5, 138.8, 137.0, 136.2, 135.3, 131.5, 130.8, 130.3, 129.3,

129.2, 128.9, 128.6, 128.3, 127.8, 126.2, 120.0, 78.2, 76.3, 42.9, 14.1, 13.0. $^{11}B\{^1H\}$ NMR (128.38 MHz, $CDCl_3$) δ: 0.95 (s, 1B, BF_2), −5,90 (s, 4B), −10.66 (br s, 12B), −13.51 (s, 4B). ESI-HRMS $[M+Na]^+$: *m/z* 1015.6956; $C_{53}H_{63}B_{21}F_2N_2Na^+$ requires 1015.6951.

Synthesis and characterization of compound 4. General procedure (**A**) starting from **1b** and ***m*-Ph-CB**. Purification by flash column chromatography on silica gel (DCM) gave **4** as a bright blue solid (52%, R_f = 0.55 DCM). ^1H NMR (600 MHz, $CDCl_3$): δ 7.38 (d, J = 8.2 Hz, 4H), 7.35 (d, J = 8.6 Hz, 4H), 7.26–7.18 (m, 8H), 7.10 (d, J = 8.1 Hz, 4H), 7.06 (d, J = 8.7 Hz, 2H), 6.88 (d, J = 16.5 Hz, 2H), 6.62 (d, J = 16.5 Hz, 2H), 4.23–4.20 (m, 2H), 3.95–3.92 (m, 2H), 3.79–3.76 (m, 2H), 3.75–3.70 (m, 2H), 3.70–3.66 (m, 2H), 3.62–3.58 (m, 2H), 3.47 (t, J = 6.8 Hz, 2H), 3.26 (s, 4H), 2.72 (s, 6H), 1.58–1.54 (m, 2H), 1.52 (s, 6H), 1.40–1.33 (m, 2H), 0.91 (t, J = 7.4 Hz, 3H). $^{13}C\{^1H\}$ NMR (150 MHz, $CDCl_3$): δ 155.2, 139.0, 137.2, 136.3, 135.4, 132.0, 130.9, 130.4, 129.6, 129.4, 128.9, 128.7, 128.4, 127.9, 127.6, 127.2, 126.3, 120.2, 115.5, 78.3, 76.4, 71.4, 71.1, 70.9, 70.8, 70.2, 69.9, 67.7, 43.0, 31.8, 29.8, 19.4, 14.1, 13.4. $^{11}B\{^1H\}$ NMR (128.38 MHz, $CDCl_3$) δ:0.93 (s, 1B, BF_2), −5.92 (s, 4B), −10.64 (br s, 12B), −13.48 (s, 4B). ESI-HRMS $[M+Na]^+$: *m/z* 1219.8335; $C_{63}H_{83}B_{21}F_2N_2O_4Na^+$ requires 1219.8318.

Synthesis and characterization of compound 5. A round-bottomed flask equipped with a reflux condenser was charged with 3 mL of dry 1,4-dioxane, and the solvent was degassed with nitrogen for 15 min. The carborane ***m*-Me-CB** (1 equiv.) and mono-iodinated BODIPY derivative **1c** (1.1 equiv.) were added, followed by $[Pd_2(dba)_3]$ (1.2 mol%), $[Pd(t\text{-}Bu_3P)_2]$ (1.6 mol%) and Cy_2NMe (1.34 equiv.). The reaction mixture was heated at reflux overnight. After complete conversion of the starting material (as monitored by TLC analysis), the mixture was filtered over celite, washed with THF and concentrated to dryness. The crude residue was purified by flash column chromatography on silica gel (PE/DCM 7/3 v/v) to give **5** as a bright purple solid (72%, R_f = 0.4 PE/DCM 7/3 v/v). ^1H NMR (600 MHz, $CDCl_3$): δ 7.53–7.46 (m, 3H), 7.36 (d, J = 8.1 Hz, 2H), 7.31–7.27 (m, 2H), 7.05 (d, J = 8.2 Hz, 2H), 6.86 (d, J = 16.5 Hz, 1H), 6.60 (d, J = 16.5 Hz, 1H), 6.00 (s, 1H), 3.16 (s, 2H), 2.71 (s, 3H), 2.57 (s, 3H), 1.46 (s, 3H), 1.37 (s, 3H). $^{13}C\{^1H\}$ NMR (150 MHz, $CDCl_3$): δ 156.1, 154.8, 143.6, 141.8, 138.7, 137.1, 136.4, 135.2, 131.9, 131.2, 130.7, 130.3, 129.3, 129.2, 128.6, 128.2, 126.2, 121.7, 120.1, 76.8, 70.8, 42.8, 24.6, 14.8, 14.6, 14.1, 13.0.

Synthesis and characterization of compound 6. To a stirred solution of **5** (0.13 mmol) in dry DCM (30 mL) under a positive N_2 atmosphere was added *N*-iodosuccinimide (NIS, 0.26 mmol, 2 eq.), and the reaction mixture was stirred at RT overnight. The mixture was then washed with water, dried over Na_2SO_4 and purified by flash column chromatography on silica gel (PE/DCM 75/25 v/v) to give **6** as purple solid (84%, R_f = 0.55 PE/DCM 75/25 v/v). ^1H NMR (600 MHz, $CDCl_3$): δ 7.48–7.43 (m, 3H), 7.30 (d, J = 8.3 Hz, 2H), 7.24–7.20 (m, 2H), 6.99 (d, J = 8.1 Hz, 2H), 6.77 (d, J = 16.5 Hz, 1H), 6.55 (d, J = 16.5 Hz, 1H), 3.10 (s, 2H), 2.65 (s, 3H), 2.58 (s, 3H), 1.56 (s, 3H), 1.34 (s, 3H), 1.31 (s, 3H). $^{13}C\{^1H\}$ NMR (150 MHz, $CDCl_3$): δ 157.2, 155.0, 143.6, 141.4, 140.3, 136.8, 136.6, 135.1, 131.5, 131.3, 130.3, 129.7, 129.4, 128.1, 126.2, 119.6, 84.8, 76.6, 70.8, 42.7, 29.8, 24.6, 16.9, 16.0, 14.3, 13.1.

Synthesis and characterization of compound 7. General procedure (**B**) starting from **6** and ***o*-Ph-CB**. Purification by flash column chromatography on silica gel (PE/DCM 6/4 v/v) gave **7** as a bright blue solid (55%, R_f = 0.35 PE/DCM 75/25 v/v). ^1H NMR (600 MHz, $CDCl_3$): δ 7.72 (d, J = 7.7 Hz, 2H), 7.57–7.50 (m, 4H), 7.49–7.43 (m, 2H), 7.38 (d, J = 8.1 Hz, 2H), 7.34–7.32 (m, 2H), 7.29 (d, J = 8.1 Hz, 2H), 7.07 (d, J = 8.0 Hz, 2H), 6.87 (d, J = 16.3 Hz, 1H), 6.85 (d, J = 16.3 Hz, 1H), 6.78 (d, J = 8.1 Hz, 2H), 6.62 (d, J = 16.5 Hz, 1H), 6.58 (d, J = 16.5 Hz, 1H), 3.18 (s, 2H), 3.07 (s, 2H), 2.73 (s, 3H), 2.72 (s, 3H), 1.64 (s, 3H), 1.47 (s, 3H), 1.46 (s, 3H). $^{13}C\{^1H\}$ NMR (150 MHz, $CDCl_3$): δ 155.4, 155.3, 141.6, 138.9, 137.4, 137.1, 136.4, 135.4, 134.5, 131.6, 131.6, 131.0, 130.9, 130.7, 130.5, 130.4, 129.4, 129.3, 129.2, 129.0, 128.9, 128.4, 126.2, 126.1, 120.3, 120.0, 83.8, 82.1, 70.8, 42.8, 40.8, 32.1, 24.7, 22.8, 14.2, 13.1. $^{11}B\{^1H\}$ NMR (128.38 MHz, $CDCl_3$) δ: 1.08 (s, 1B, BF_2), −3.17 (s, 2B), −6.22 (s, 1B), −7.98 (s, 1B), −10.24 (br s, 14B), −12.93 (s, 2B). ESI-HRMS $[M+Na]^+$: *m/z* 953.6817; $C_{48}H_{61}B_{21}F_2N_2Na^+$ requires 953.6794.

Synthesis and characterization of compound 8. General procedure (**B**) starting from **6** and ***m*-Ph-CB**. Purification by flash column chromatography on silica gel (PE/DCM 7/3 v/v) gave **8** as a bright blue solid. (35%, R_f = 0.21 PE/DCM 7/3 v/v). ^1H NMR (600 MHz, $CDCl_3$): δ 7.53 (m, 3H), 7.38–7.33 (m, 9H), 7.23–7.21 (m, 2H), 7.10–7.06 (m, 4H), 6.87 (d, J = 16.5 Hz, 2H), 6.62 (d, J = 16.5 Hz, 2H), 3.26 (s, 2H), 3.18 (s, 2H), 2.74 (s, 6H), 1.64 (s, 3H), 1.47 (s, 6H). $^{13}C\{^1H\}$ NMR (150 MHz, $CDCl_3$): δ 155.4, 141.6, 138.9, 137.1, 137.1, 136.4, 136.3. 135.4, 132.0, 131.0, 130.9, 130.4, 129.4, 129.3, 129.0, 128.7, 128.4, 127.9, 126.3, 126.2, 121.0, 120.0, 78.3, 76.8, 76.3, 70.9, 43.0, 42.8, 24.7, 14.2, 13.1. $^{11}B\{^1H\}$ NMR (128.38 MHz, $CDCl_3$) δ: 1.01 (br s, 1B, BF_2), −6.05 (s, 3B), −7.85 (s, 1B), −10.46 (s, 12B), −13.01 (s, 4B). ESI-HRMS $[M+Na]^+$: *m/z* 953.6824; $C_{48}H_{61}B_{21}F_2N_2Na^+$ requires 953.6794.

Synthesis and characterization of compound 9. General procedure (**A**) starting from **1d** and ***m*-Ph-CB**. Purification by flash column chromatography on silica gel (PE/DCM 7/3 v/v) gave **9** as a bright blue solid. (30%, R_f = 0.33 PE/DCM 7/3 v/v). ^1H NMR (600 MHz, $CDCl_3$): δ 7.79 (d, J = 16.3 Hz, 2H), 7.62 (d, J = 8.1 Hz, 4H), 7.56–7.50 (m, 6H), 7.37–7.36 (m, 4H), 7.32 (d, J = 16.3 Hz, 2H), 7.25–7.21 (m, 5H), 7.19 (d, J = 8.1 Hz, 4H), 6.93 (d, J = 4.5 Hz, 2H), 6.82 (d, J = 4.4 Hz, 2H), 3.30 (s, 4H). $^{13}C\{^1H\}$ NMR (150 MHz, $CDCl_3$): δ 154.8, 139.8, 138.0, 136.4, 136.2, 135.9, 135.3, 134.4, 130.6, 130.5, 130.0, 129.9, 128.7, 128.4, 127.9, 129.9, 119.7, 116.5, 78.4, 76.1, 43.1. ESI-MS $[M+H]^+$: *m/z* 939.16.

2.4. Photophysical measurements

The optical properties were evaluated in anhydrous grade THF, MeOH, CH_3CN, $CHCl_3$, toluene, dioxane, DMSO purchased from Sigma Aldrich and used without further purifications. Binary mixtures of MilliQ water in THF at different ratios (20, 40, 60 and 80% v/v) were prepared to evaluate the probes' solubility in water and the photophysical responses in aqueous media. Stock solutions in the selected solvent with a concentration between $2.87*10^{-4}$ M and $3.73*10^{-4}$ M were prepared for all the compounds tested. UV–Vis spectra were recorded on VARIANT Cary 5 UV–Vis–NIR spectrophotometer. Molar extinction coefficients were determined with solutions of THF with concentrations in the range $0.20*10^{-5}$ M to $1.50*10^{-5}$ M. Emission spectra have been recorded with a VARIANT Cary Eclipse Fluorescence spectrophotometer. The excitation wavelengths were set just before the respective absorption maxima in each solvent tested to provide adequate excitation energy and maximize the detected signal, excitation and the emission slits are set at 2.5 nm. The samples concentration was adjusted to have an absorbance between 0.1 and 1 at the Abs_{max} to evaluate the general photophysical properties in THF (Abs_{max}, Em_{max}, Φ_F and Stokes Shift) and the possible solvatochromic features in MeOH, CH_3CN, $CHCl_3$, toluene, dioxane, DMSO. All the measurements were carried out in a 1 cm four-sided quartz cuvette from Hellma Analitics. The absorption and steady state emission spectra were corrected for their respective blank. No fluorescent contaminants were detected on excitation in the wavelength region of experimental interest.

The Fluorescence quantum yield evaluation was carried out on samples with concentrations adapted to have an absorbance lower than 0.1 in THF at the excitation wavelength (λ_{ex}) using the above-mentioned DMSO stock solutions. The fluorescence quantum yield (ϕ) were evaluated compared on an external standard, Rhodamine 101 (ϕ:1 in MeOH, λ_{ex} 576 nm) [27] by applying the following equation:

$$\varphi = \varphi_{STD}\frac{I}{I_{STD}}\frac{Abs_{STD}}{Abs}\frac{n^2}{n^2_{STD}} \quad (1)$$

where ϕ_{STD} is the fluorescence quantum yield of the standard, I and I_{STD} are the integrated area of the emission band of the sample and the standard respectively. Abs and Abs_{STD} are the absorbance at the excitation wavelength for the sample and the standard, respectively. *n* and

n_{STD} are the solvent refractive index of the sample and the standard solutions, respectively.

2.5. Computational details

The structures were optimized by using the Coulomb-attenuated B3LYP functional (CAM-B3LYP) [28] with the Pople's 6-31G(d) basis set [29]. The solvent (THF) was simulated within the Solvation Model based on Density (SMD) [30] and Integral Equation Formalism-Polarizable Continuum Model (IEF-PCM) schemes [31]. Excitation energies were calculated by single point time dependent-DFT calculations [32], using the O3LYP functional [33] and the same basis set of the optimizations. All the calculations were carried out using the GAUSSIAN 16 system of programs [34]. Figures were obtained with the graphical program GaussView [35].

3. Results and discussion

3.1. Synthesis and characterization of dyes

The presence of halogen atoms, either directly on the BODIPY core or attached to an aryl ring, facilitates further extension of the π-conjugation and to build sophisticated structures by means of metal-catalyzed coupling reactions [36]. Based on our previously reported results on the functionalization of the (aza)BODIPY core with C_c-substituted styrenyl-containing *o*- or *m*-carborane derivatives [20], we started our preliminary investigation by testing the Heck coupling procedure on the 2,6-diiodo-BODIPY derivative **1a** and the methyl substituted styrenyl *m*-carborane ***m*-Me-CB** (Scheme 1). The 2,6-diiodo-1,3,5,7-tetramethyl-BODIPY dye **1a**, synthesized by condensation of 2,4-dimethylpyrrole with benzaldehyde followed by mild iodination with I_2/HIO_3 [37], exhibits an absorption maxima at 534 nm and a negligible fluorescence quantum yield due to the high heavy atom-induced intersystem crossing (ISC) at the excited state [38]. The ***m*-Me-CB** has been easily synthesized by electrophilic trapping of the parent lithium-*closo*-carborane cluster with 4-vinylbenzyl chloride as previously reported [12l].

The 2,6-diiodoBODIPY **1a** was reacted with two equivalents of ***m*-Me-CB** in refluxing 1,4-dioxane using the $[Pd_2(dba)_3]$ (3 mol%) and $[Pd(t\text{-}Bu_3P)_2]$ (6 mol%) catalytic system [39], in the presence of Cy_2NMe as a base. Under these conditions, the reaction proceeded smoothly in 12 h with full conversion of the starting materials affording the target compound **2** in 43% isolated yield (β,β-isomer). Successful incorporation of the carborane cage was easily confirmed by the presence of the BH broad band in the upfield region of the ^{1}H NMR (Fig. 2, top). Additionally, protons from C_c-CH_3 are identified near 1.65 ppm, which was consistent with the *m*-Me substitution pathway of the carborane cage. The ^{1}H NMR spectrum confirmed the symmetric structure of the dye, showing the benzylic protons signal of the spacer at 3.18 ppm and the two equivalent methyl signals of the fluorophore scaffold at 2.74 and 1.47 ppm. Moreover, analysis of the coupling constant for the olefinic proton doublets at 6.87 ppm and 6.63 ppm revealed the full *trans*-selectivity of the cross coupling reaction ($^3J_{HH} = 16.5$ Hz). Although the formation of geminal substituted olefins in the cationic Heck reaction of 4-substituted styrenes should be suppressed by the presence of the strong electron-withdrawing carboranyl cage [40], a small amount of α,β-isomer **2a** (6%) was also isolated from the reaction mixture, while no α,α-isomer was detected (Scheme 1) [23]. The presence of both the terminal olefinic protons (5.84 ppm and 5.10 ppm respectively, $^2J_{HH} = 1.3$ Hz) and the more deshielded *trans*-olefinic protons ($^3J_{HH} = 16.5$ Hz) in the ^{1}H NMR spectrum of **2a** (Fig. 2, bottom) revealed the asymmetric substitution pathway, alongside with the splitting of the four methyl groups of the BODIPY unit.

Analysis of the $^{11}B\{^1H\}$ NMR spectra further confirmed the formation of the expected compounds, showing one resonance centered at 0.99 ppm for β,β-isomer **2** and at 1.01 ppm for α,β-isomer **2a** assigned to the -BF_2 unit (see $^{11}B\{^1H\}$ NMR spectra in the SI). In addition to the -BF_2 resonance, these compounds show broad resonances in the region from −6.17 to −13.04 ppm with the typical 1:1:6:2 pattern characteristic of *m*-carborane clusters [12f]. The $^{13}C\{^1H\}$ NMR spectrum of β,β-isomer **2** shows a resonance at 42.8 ppm assigned to the two equivalent benzylic carbon atoms (split into two different signals at 42.7 and 42.6 ppm for the asymmetric α,β-isomer **2a**), and the C_c-CH_3 can be identified from

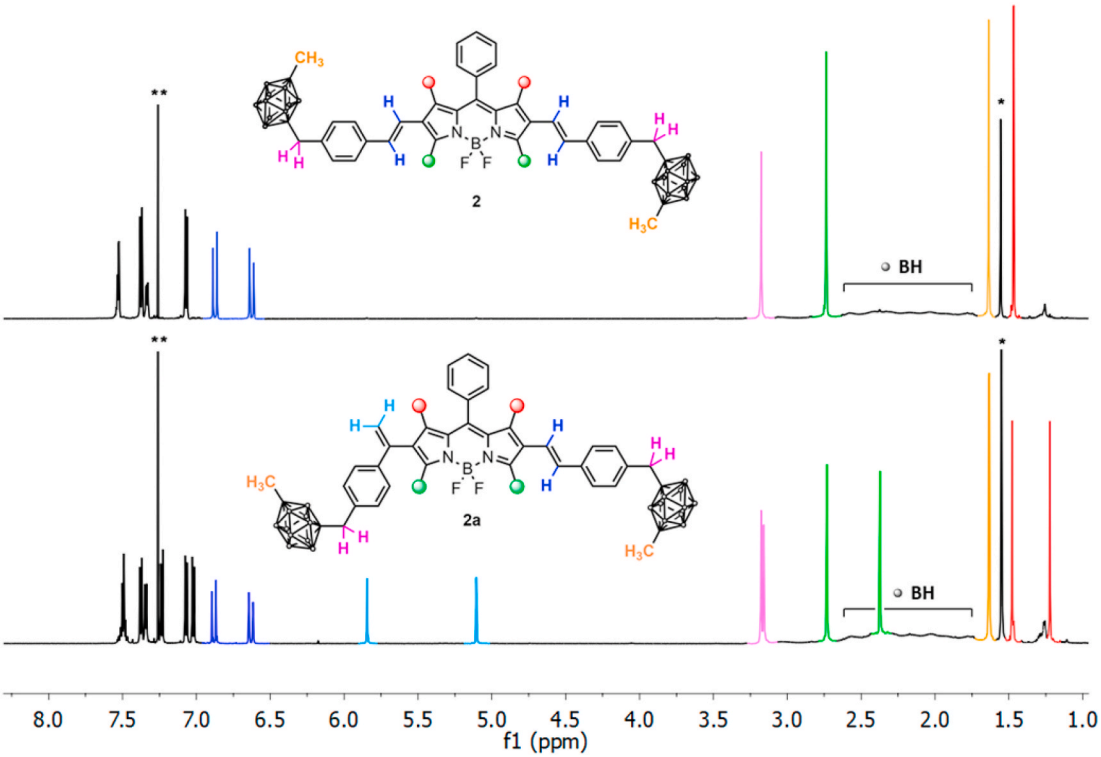

Fig. 2. ^{1}H NMR spectra of bis-β,β-styrenyl carborane BODIPY derivative **2** (top) and its α,β-isomer **2a** (bottom) in $CDCl_3$. *H_2O signal; ** residual $CDCl_3$ peak.

24.0 to 25.0 ppm for both isomers (see $^{13}C\{^1H\}$ NMR spectra in the SI).

The Heck coupling procedure was successfully applied to the styrenyl substituted *m*-carborane derivative ***m*-Ph-CB** bearing a phenyl ring at one C atom of the cluster (C_c) to achieve symmetric dyes **3** and **4** (Scheme 2). To our delight, the reaction of iodinated BODIPY **1a** using two equivalents of ***m*-Ph-CB** as coupling partner proceeded smoothly in the presence of $[Pd_2(dba)_3]$ (3 mol%), $[Pd(t\text{-}Bu_3P)_2]$ (6 mol%), Cy_2NMe (5 eq.) in refluxing 1,4-dioxane, affording the corresponding dye **3** in 57% isolated yield. Also halogenated BODIPY dyes **1b**, incorporating a nonionic amphiphile oligoethylene glycol alkyl chain at the *meso*-position [41], was successfully reacted with two equivalents of ***m*-Ph-CB** derivative under the same reaction conditions affording dye **4** in 52% isolated yield. The ^1H NMR spectra clearly confirmed the symmetric structure of the dyes and the incorporation of the carborane cage, showing the typical BH broad band of the *closo*-carborane cluster in the upfield region and the benzylic protons signal of the spacer at 3.18 (**3**) and 3.26 ppm (**4**) (see ^1H NMR spectra in the SI). The $^{11}B\{^1H\}$ NMR spectra of these compounds exhibited a resonance at 0.93 ppm (**3**) and at 0.95 ppm (**4**) attributed to the -BF_2 unit, alongside with broad resonances in the region from −5.90 to −13.51 ppm with the typical 2:6:2 pattern of *m*-carborane clusters (see $^{11}B\{^1H\}$ NMR spectra in the SI).

As a further application of this methodology, we then envisaged the possibility to extend the feasibility of our approach to the synthesis of asymmetric compounds bearing two different C-substituted carborane units. We thus planned a tandem cross coupling/iodination/cross coupling approach starting from the mono-iodinated 1,3,5,7-tetramethylBODIPY dye **1c** (Scheme 2). Reaction of BODIPY **1c** with a stoichiometric amount of the *m*-substituted styrenyl-carborane ***m*-Me-CB** in the presence of $[Pd_2(dba)_3]$ (1.2 mol%), $[Pd(t\text{-}Bu_3P)_2]$ (1.6 mol%), Cy_2NMe (1.4 eq.) in refluxing dry 1,4-dioxane afforded the corresponding mono-substituted derivative **5** in good yield (72%), which was easily converted into a new potential coupling partner **6** by mild iodination at the 6-position in the presence of *N*-iodosuccinimide (NIS, 2 equiv.) at room temperature overnight. Although the final Heck coupling between substrate **6** and styrenyl-carboranes ***o*-Ph-CB** and ***m*-Ph-CB** required a higher catalyst loading (5 mol% of $[Pd_2(dba)_3]$ and $[Pd(t\text{-}Bu_3P)_2]$, asymmetric dyes **7** and **8** were successfully isolated with moderate yields of 55% and 35%, respectively. Analysis of the ^1H NMR spectra (see ^1H NMR spectra in the SI) revealed the asymmetric substitution pathway, showing two different benzylic signals of the spacers at 3.18 and 3.07 ppm (**7**) and at 3.26 and 3.18 (**8**). Moreover, the ^1H NMR of **7** exhibited two resolved *trans*-olefinic systems belonging to the different styrenyl carborane units ($^3J_{HH} = 16.3$ Hz and $^3J_{HH} = 16.5$ Hz), confirming the stereoselectivity of each Heck coupling reaction of the tandem sequence. The $^{11}B\{^1H\}$ NMR spectrum of **7**, bearing two different carborane isomers, one *m*- and one *o*-carborane, displayed the -BF_2 unit centered at 1.08 ppm and a set of broad resonances in the range from −3.17 to −12.93 ppm, with a 2:1:1:14:2 pattern reflecting the combined *m*- (1:1:6:2) and *o*- (2:8) typical distributions of *closo*-carboranes. Analysis of the $^{11}B\{^1H\}$ NMR spectrum of **8** showed a resonance of the -BF_2 unit at 1.01 ppm and the 1:1:6:2 pattern of broad resonances in the region from −6.05 to −13.01 ppm, ascribed to the two Me and Ph-substituted *m*-carborane clusters (see $^{11}B\{^1H\}$ NMR spectra in the SI).

With the aim to compare the photophysical properties of this new class of red-shifted 2,6-disubstituted carborane-BODIPY dyes with other similar dyes with different substitution patterns, we finally envisaged the possibility to exploit our synthetic methodology for the introduction of two styrenyl-containing carboranes on the BODIPY core at the 3,5-positions. To this purpose, we planned a short one-step synthesis of the symmetric dye **9** bearing two ***m*-Ph-CB** units starting from the corresponding 3,5-dichloroBODIPY **1d** (Scheme 3). The 3,5-dichloro-*meso*-phenyl-BODIPY dye **1d** was synthesized by acidic condensation of pyrrole with benzaldehyde followed by chlorination/oxidation, and exhibits an absorption maxima centered at 517 nm ($\Phi_F = 0.13$) [42]. Pleasingly, the 3,5-dichloroBODIPY **1d** reacted smoothly in 12 h with two equivalents of ***m*-Ph-CB** in refluxing 1,4-dioxane under our Heck coupling conditions, affording the desired 3,5-disubstituted BODIPY **9** in 30% isolated yield. More details about the structural characterization of all the compounds can be found in the Supporting Information.

3.2. Photophysical properties

The photophysical behavior of the final compounds was investigated, and the most significant spectroscopic properties are collected in Table 1. Fig. 3 shows UV/Vis and fluorescence spectra of dyes in THF solution at 298 K. The optical properties of the new synthesized compounds were compared with the parent 2,6-styrenyl disubstituted BODIPY dye **DS-BDP** (*meso*-phenyl-2,6-distyrylBODIPY) [23] and the 3,5-styrenyl disubstituted BODIPY analogue **3,5-BDP** (*meso*-phenyl-3,5-distyrylBODIPY) [43], both lacking the carborane cages.

Generally, the absorption spectra of 2,6-disubstituted compounds **2–4** and **7–8** exhibited a significant bathochromic shift compared to their parent fluorophore scaffolds (*meso*-phenyl-1,3,5,7-tetramethyl BODIPY, $\lambda_{abs} = 500$ nm in THF) [44], but slightly red-shifted (3–9 nm) with respect to the **DS-BDP** (*meso*-phenyl-2,6-distyrylBODIPY) [23], showing a very small influence of the carborane cage and their respective C_c-substituents (Me or Ph). Overall, the fluorescence quantum yields of the new synthesized compounds **2–4** and **7–8** are lower compared to other BODIPY derivatives [17a], whereas all the compounds showed an enhanced fluorescence emission efficiency compared to the reference compound **DS-BDP** (Table 1).

Moreover, compounds **2–4** and **7–8** showed large Stokes shifts (56–65 nm) compared to other BODIPY dyes, which suffer of some experimental limitations such as self-quenching [45]. The simplest symmetrical BODIPY derivative **2**, containing the ***m*-Me-CB** unit, showed the highest fluorescence quantum yield ($\Phi_F = 0.14$) of the series bearing a phenyl group at the *meso*-position (Table 1, entry 2). The photophysical features of **2** are easily distinguishable from the side product **2a** containing one α-styrenyl substituted unit. A remarkable hypsochromic shift in the absorption (548 nm) and emission (627 nm) spectra of **2a** in THF was observed (Table 1, entry 3), together with a larger Stokes shift and a significantly lower Φ_F, compared to the β,β-isomer **2**. These differences can be readily attributed to the lower degree of conjugation between the α-styrenyl substituent and the BODIPY scaffold, and suggest an increased HOMO-LUMO gap as previously reported by Li and Shen [23]. The introduction of a phenyl ring on the same *m*-carborane isomer in **3** had minimal to no effect on the photophysical features of the compound (Table 1, entry 4), which were depicted by comparable λ_{abs}, λ_{em}, whereas a slight drop of the Φ_F was observed ($\Phi_F = 0.11$). When Ph-substituted *m*-carborane derivatives were compared (**3** and **4**), a slight increase of the fluorescence efficiency ($\Phi_F = 0.14$) was produced by introducing a short-terms oligoethylene glycol alkyl chain on the *meso*-phenyl ring (**4**, Table 1, entry 5). This latter was of particular synthetic value since it allowed the design of pre- or post-functionalization strategies for the introduction of amphiphilic solubilizing groups on the fluorophore core without affecting the PL properties. The replacement of one ***m*-Me-CB** in **2** with a different CB moiety (***o*-Ph-CB** for compound **7** or ***m*-Ph-CB** for compound **8**) had no significant impact on the photophysical features as expected. Regarding the asymmetric BODIPY dyes **7** and **8**, similar results were obtained for both compounds (Table 1, entries 6–7), exhibiting comparable photophysical features in the series, although slightly lower quantum efficiencies were obtained when compared to their symmetric analogues **2–4**. Interestingly, shifting the styrenyl substituents to the 3,5-positions of the BODIPY core caused a remarkable effect on the photophysical properties of the dyes. The absorption spectrum of compound **9** (Fig. 3, right), bearing two Ph-substituted *m*-carborane units at the 3,5-positions of the fluorophore, exhibited the typical narrow and intense structured $S_0 \rightarrow S_1$ transition with $\lambda_{abs} = 641$ nm, slightly red-shifted (8 nm) with respect to the reference compound **3,5-BDP** (*meso*-phenyl-3,5-distyrylBODIPY, $\lambda_{abs} = 633$ nm). The absorption maxima of **9** (641 nm) was

Table 1
Selected photophysical data for the reported compounds **2**, **2a**, **3**, **4** and **7–9**.[a] BODIPY dyes **DS-BDP** (entry 1)[b] and **3,5-BDP** (entry 9)[c] were added for comparison.

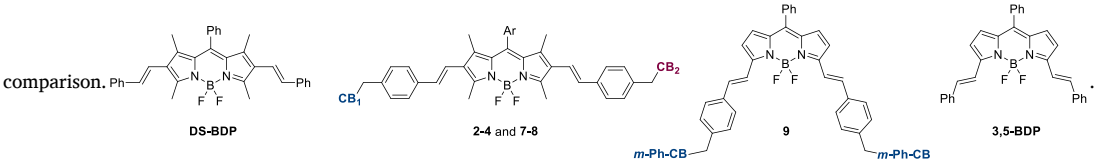

Entry	Compound	λ_{abs} (nm)	λ_{em}(nm)	$\varepsilon/10^6$ (M^{-1} cm^{-1})	Φ_F[d]	Stokes shift/10^3 (cm^{-1})	ε Φ_F (M^{-1} cm^{-1})
1	**DS-BDP**	575	633	0.031	0.01	1.59	310
2	**2**	584	640	0.056	0.14	1.50	7840
3	**2a**	548	627	0.030	0.05	2.30	1500
4	**3**	578	643	0.035	0.11	1.75	3850
5	**4**	580	640	0.029	0.14	1.62	4060
6	**7**	578	643	0.049	0.12	1.75	5880
7	**8**	582	641	0.058	0.12	1.58	6960
8	**9**	641	651	0.087	0.36	0.24	31320
9	**3,5-BDP**	633	646	0.104	0.83	0.32	86320

[a] Measured in THF at room temperature.
[b] Data for **DS-BDP** are reported in the literature in CH_2Cl_2 (see ref. [23]).
[c] Data for **3,5-BDP** are reported in the literature in THF (see ref. [43]).
[d] Fluorescence quantum yields were determined using solutions of Rhodamine 101 in methanol ($\Phi_F = 1$) as standard [27].

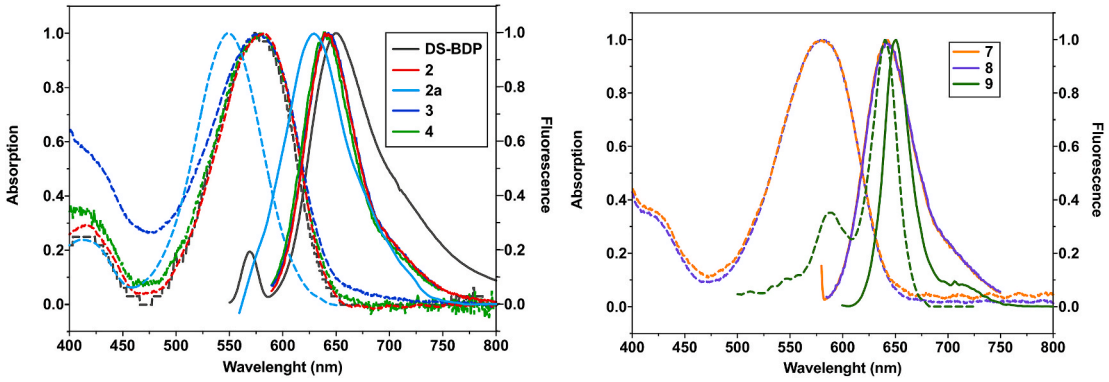

Fig. 3. Normalized absorption (dashed) and emission (solid) spectra of symmetric (**DS-BDP** and **2–4**, left), asymmetric (**7–8**, right) and **9** (right) carborane-BODIPY derivatives in THF.

largely red-shifted in comparison to its 2,6-disubstituted analogue **3** (578 nm), suggesting a more planar conformation characterized by a higher extinction coefficient (Table 1, entry 8). The emission maxima of **9** was slightly red-shifted compared to **3** (8 nm) and reference compound **3,5-BDP** (5 nm), while **9** showed a smaller Stokes shift compared to the 2,6-disubstituted analogue **3** and **3,5-BDP** in THF. Generally, 3,5-distyrenyl substituted BODIPY dyes show higher fluorescence quantum yields compared to their 2,6-analogues (see Table 1, entries 1 and 9, and reference [23]) due to a lower rate of nonradioactive decay. Compound **9** showed a higher fluorescence quantum yield ($\Phi_F = 0.36$, Table 1 entry 8) compared to the corresponding 2,6-disubstituted dye **3** ($\Phi_F = 0.11$, Table 1 entry 4), however significantly lower with respect to **3,5-BDP** (Table 1, entry 9). We have also calculated the brightness of these dyes, which is the product of the molar extinction coefficient at the excitation wavelength and the fluorescence quantum yield [$\varepsilon(\lambda)\cdot\Phi_F$]. As expected, the 3,5-disubstituted compound **9** showed the highest brightness of the series (31320 M^{-1} cm^{-1}), while among the 2,6-substituted dyes the highest value of brightness was found for BODIPY derivative **2** (7840 M^{-1} cm^{-1}), followed by the asymmetric derivatives **8** (6960 M^{-1} cm^{-1}) and **7** (5880 M^{-1} cm^{-1}).

3.3. Theoretical calculations

Theoretical calculations have been performed with the Gaussian 16 software package on symmetric *m*-Ph styrenyl carborane disubstituted dyes **3**, **9**, and reference compounds **DS-BDP** and **3,5-BDP** to account for some of the observed photophysical properties (see section 2.5 for computational details). The results are summarized in Table 2, which highlight the calculated characteristics of the electronic transitions responsible for the lowest-energy bands. The molecular orbitals HOMO and LUMO involved in the electronic transitions are illustrated in Fig. 4, and the optimized geometries of compounds **3** and **9** for the ground state (S_0) and the first excited state (S_1) are shown in Fig. 5.

The theoretical calculation results were in good accordance with the observed experimental data, and the absorption maxima of the lowest-energy bands were mainly assigned to $\pi\rightarrow\pi^*$ type $S_0\rightarrow S_1$ transitions involving the frontier molecular orbitals HOMOs and LUMOs.

Table 2
Calculated electronic excitation energies, oscillator strengths and the related wave functions for $S_0\rightarrow S_1$ transitions. Electronic transition data obtained by O3LYP/6-31G(d)//CAM-B3LYP/6-31G(d) for compounds **3**, **9** and references compounds **DS-BDP**[a] and **3,5-BDP**.

	E (eV)	λ (nm)	*f*	Wave function	Exp. λ (nm)
3	2.13	582	0.83	H→L (93%), H-2 →L (7%)	578
9	2.02	613	1.06	H→L (100%)	641
DS-BDP	2.22	559	0.68	H→L (92%), H-2 →L (8%)	575
3,5-BDP	2.06	603	0.99	H→L (100%)	633

[a] Experimental data for **DS-BDP** are reported in the literature in CH_2Cl_2 (see ref. [23]).

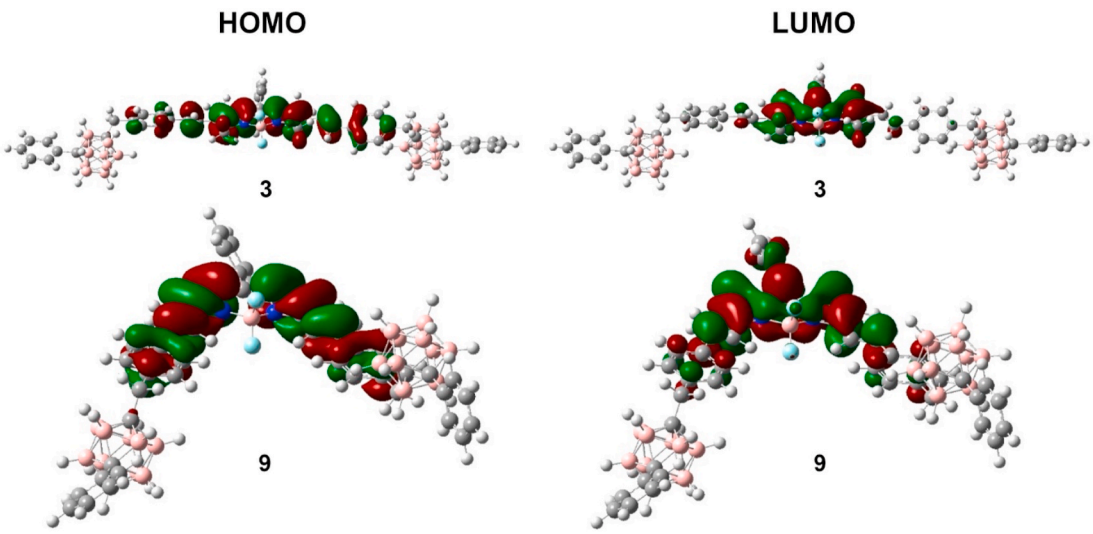

Fig. 4. CAM-B3LYP/6-31G(d) molecular orbitals HOMO (left) and LUMO (right) of carborane-BODIPY dyes **3** (top) and **9** (bottom).

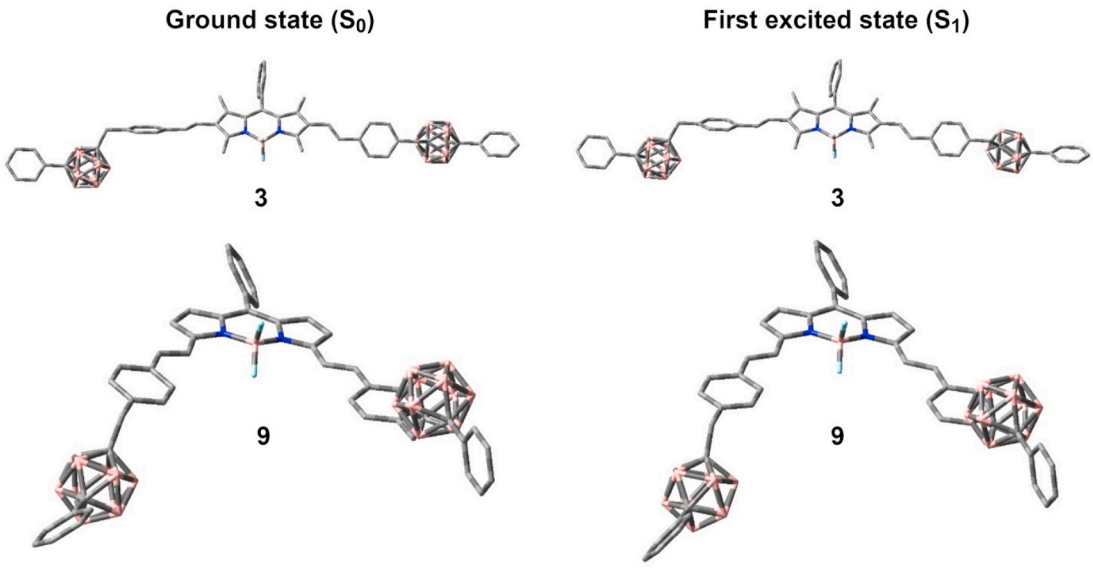

Fig. 5. CAM-B3LYP/6-31G(d) optimized geometries of the ground states (left) and the first excited states (right) of carborane-BODIPY dyes **3** (top) and **9** (bottom). Hydrogen atoms were omitted for clarity.

The calculated wavelength for the maximum of absorption for carborane-BODIPY dye **3** was 582 nm (oscillator strength $f = 0.827$), corresponding almost exclusively to the HOMO→LUMO transition (93% contribution, Table 2). Analogously, the predicted lowest-energy band of carborane-BODIPY **9** lies at 613 nm ($f = 1.063$) and arise exclusively from the HOMO→LUMO transition. This picture is consistent and comparable with the results obtained for 2,6- and 3,5- distyrenyl substituted BODIPY dyes **DS-BDP** [23] and **3,5-BDP**.

As mentioned above, 2,6-disubstituted dye **3** shows a lower fluorescence quantum yield ($\Phi_F = 0.11$, Table 1 entry 4) compared to compound **9** ($\Phi_F = 0.36$, Table 1 entry 8). Analysis of the frontier MOs for compound **3** revealed a significant contribution of the styrenyl moiety in the HOMO, while the LUMO is centered almost exclusively on the fluorophore (Fig. 4, top). This picture suggests a significant charge transfer (CT) process from the styrenyl groups to the fluorophore in the $S_0 \rightarrow S_1$ transitions, responsible for the low fluorescence efficiency observed. On the other hand, compound **9** shown significant MO coefficients on the styrenyl moieties both for the HOMO and LUMO (Fig. 4, bottom), limiting the scope for a CT fluorescence quenching.

Analysis of the optimized geometries of the ground (S_0) and excited (S_1) states of compounds **3** and **9** gave further insights into the experimental observed photophysical properties of the disubstituted dyes. As shown in Fig. 5, the main difference between 2,6- (compound **3**) and 3,5- (compound **9**) disubstituted dyes relies in the level of coplanarity both in the ground state and excited state geometries. The mean dihedral angles measured between the styrenyl units and the fluorophore core in the S_0 and S_1 states (Table 3) clearly evidence a significant loss in coplanarity in the ground state for compound **3** ($\theta\ S_0 = 28.8°$), which is slightly lower in the S_1 surface ($\theta\ S_1 = 23.1°$), due to the steric hindrance of the

Table 3
Mean dihedral angles (θ) for compounds **3**, **9**, **DS-BDP** and **3,5-BDP** in the ground state (S_0) and excited state (S_1).

	Compound			
	3	**9**	**DS-BDP**	**3,5-BDP**
θ (S_0)	28.8°	9.9°	31.6°	10.4°
θ (S_1)	23.1°	3.9°	22.6°	5.4°

four methyl groups on the BODIPY moiety. Compound **9** shows a greater level of coplanarity both in ground and in excited state geometries, with measured mean dihedral angles of 9.9° for S_0 and 3.9° for S_1 state. Comparable results were obtained for reference compounds **DS-BDP** (31.6° for S_0 and 22.6° for S_1 states) and **3,5-BDP** (10.4° for S_0 and 5.4° for S_1 states). Overall, the presence of the carborane units has a little effect on the coplanarity of the states. However, the introduction of the carborane cage in the 2,6-positions of the fluorophore (compound **3**) induces a slightly higher degree of coplanarity in the S_0 and S_1 states, suggesting a possible explanation for the higher fluorescence efficiency observed for **3** ($\Phi_F = 0.14$) compared to the reference compound **DS-BDP** ($\Phi_F = 0.01$). On the other hand, the coplanarity of the states for 3,5-disubstituted dyes is rather unaffected by the presence of the carborane units. Unfortunately, theoretical calculations have not given a rational explanation to the decrease of Φ_F for compound **9** with regards to the reference **3,5-BDP**. We are not able to stablish a clear relationship between the introduction of the carborane cluster and the quenching of the emission efficiency.

The mean dihedral angle values clearly rationalize the larger Stokes shifts observed for compound **3** compared to the 3,5-disubstituted compound **9** (see Table 1, entries 4 and 8) [46]. Moreover, the loss in coplanarity due to steric interactions observed for compound **3** may enhance the formation of conical intersections between a charge-separated non-emissive S_1 state and the ground state [47]. This aspect, together with the frontier MOs analysis, accounts for the lower fluorescence efficiencies observed for 2,6-distyrenyl BODIPY dyes compared to their 3,5-disubstituted analogues.

3.4. Solvatochromic effects

The most performing probes have been also investigated in different solvents to evaluate their solubility, spot potential aggregation issues and screen the photophysical properties related to various polar environments. Of these, the polarity-induced change in the optical properties, often denoted as fluorescence solvatochromism [48], is of wide interest in order both to identify several polarity-dependent molecular events, and in advancing the design of novel functional dyes. Among the new compounds, one representative candidate for each class was selected on the basis of the most promising optical features (Φ_F and brightness). The UV–Vis absorption and fluorescence spectra of carborane-BODIPY dyes **2** (*m*-Me symmetric), **3** (*m*-Ph symmetric), **7** (asymmetric) and 3,5-disubstituted analogue **9** were recorded in solvents with different dielectric constants (2.25–46.7) at 298 K (Fig. 6). The scarce influence of solvent polarity observed on the absorption spectra of the new compounds reflected the typical photophysical behavior of BODIPY chromophores [49].

Compound **2** showed a weak dependence of the absorption (575–584 nm) and the emission (642–652 nm) maxima on the environmental polarity (Fig. 6a), as expected in symmetrical scaffolds due to the lack of an intrinsic molecular dipole moment. As a consequence, a similar behavior was observed for compound **3** bearing the phenyl substituted *m*-carborane cage, showing very little solvent effects on the absorption maxima (572–581 nm) and fluorescence emission maxima slightly modulated in the 640–650 nm range (Fig. 6b). The introduction of two different substituted *o*- and *m*-carborane units in the fluorophore core did not affect significantly the intrinsic molecular dipole moment of asymmetric carborane-BODIPY dyes, as a matter of fact the influence of

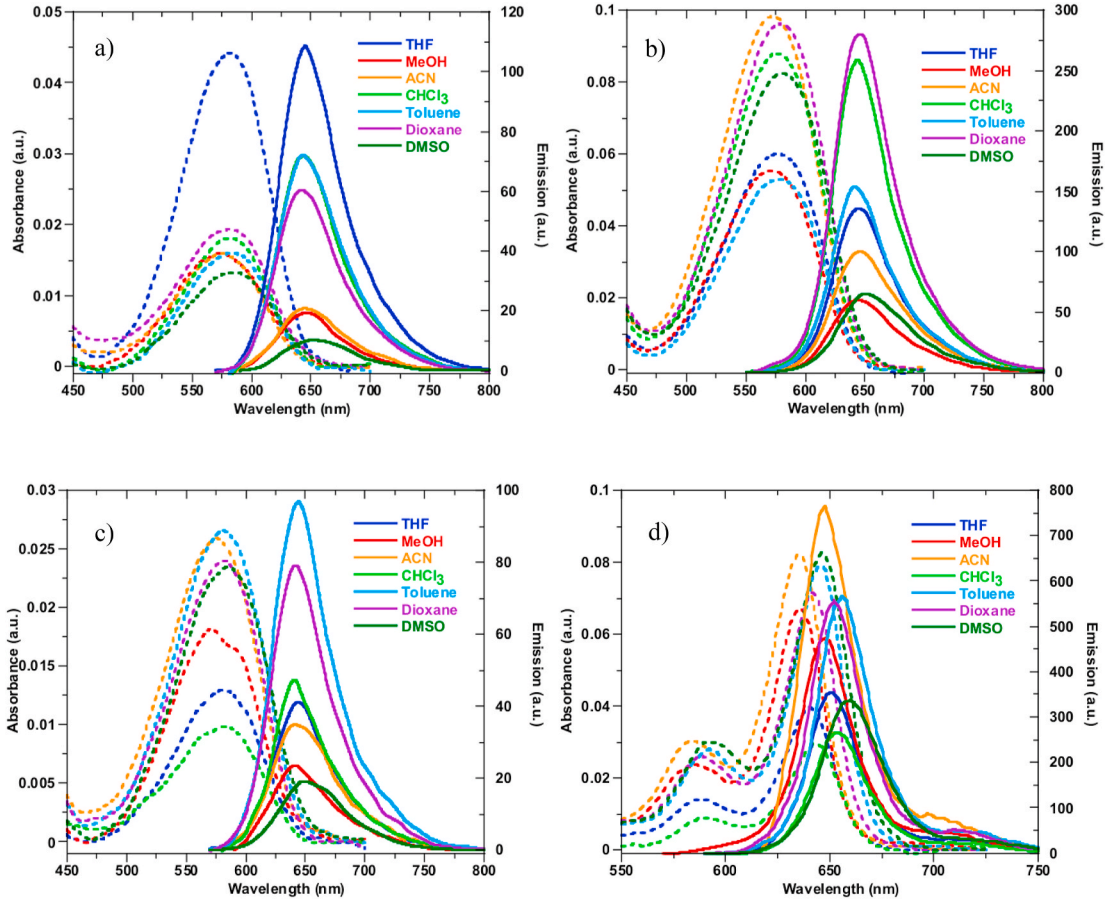

Fig. 6. UV–Vis absorption and fluorescence spectra of BODIPY dyes (a) **2**, (b) **3**, (c) **7** and (d) **9** recorded in different solvents (ε) at 298 K: dioxane (2.25), toluene (2.38), $CHCl_3$ (4.81), THF (7.58), CH_3OH (32.7), CH_3CN (37.5), and DMSO (46.7). See Supporting Information for normalized spectra.

solvent polarity on the PL properties of **7** (Fig. 6c) remained very small (λ_{abs} = 572–584 nm and λ_{em} = 640–650 nm). A similar behavior was observed for the symmetric compound **9** (Fig. 6d), as a consequence of the low molecular dipole moment. None of the investigated compounds had shown precipitation in different solutions or aggregation phenomena detectable by absorption or emission spectroscopies. The photophysical behavior in a water environment has been also investigated for compound **3** and its analogue **4**, which incorporates a short-terms oligoethylene glycol alkyl chain on the *meso*-phenyl ring. For this purpose, a series of measurements in THF, with an increasing amount of water, have been investigated and the results are shown in Fig. 7. Both probes showed a similar photophysical fingerprint in response to an increasing amount of water. Up to 40% of water in THF, the absorption spectra were characterized by a hypochromic effect while the emission traces, normalized for the absorbance intensity at excitation wavelength, showed clear profiles comparable to those observed in pure THF. In water-predominant binary mixtures (60% and 80% of water), the absorption spectra showed large, red-shifted peaks suggesting the formation of aggregates, and the emission bands were weak most likely due to aggregation phenomena. This picture is consistent with the low emission intensity of the dyes observed in polar media (see Fig. 6). However, since a clear signal in pure water is detectable in the absorption spectra, suggesting the presence of stable soluble aggregates, we speculate that these dyes might behave as fluorogenic probes. The fluorescence features might get restored upon binding or intercalation events with biological relevant molecules, making these dyes as promising candidates for further investigations in bio-supramolecular assays. Experiments aimed at evaluating both the internalization of the new dyes in several cell lines and the development of liposomal formulations are currently ongoing, and the results will be reported in due course.

4. Conclusions

In summary, a set of new red-light emitting 2,6-distyrenyl-substituted carborane-BODIPY dyes with enhanced boron content was successfully synthesized by a versatile Pd-catalyzed Heck coupling reaction, starting from a styrenyl-containing carborane and a halogenated dipyrromethene fluorophore. The synthetic procedure was successfully applied to different types of carborane derivatives with moderate yields, allowing both the introduction of two identical carborane cages into the fluorophore core and the extension of the π-conjugation within a single synthetic step. Of particular synthetic value, this methodology allowed the preparation of asymmetric dyes, bearing two different substituted carborane cages, by means of a tandem cross coupling/iodination/cross coupling sequence. The final compounds were fully characterized and their photophysical behavior was investigated. Absorption and photoluminescence (PL) emission patterns of synthesized dyes were almost unaffected by the different substituents on the C_c atom of the carborane cage or the cluster isomer. The fluorescence efficiencies of the 2,6-distyrenyl BODIPY dyes are significantly lower than those of their 3,5-disubstituted analogues. This behavior can be rationalized on the basis of the molecular orbitals involved in the main one-electron transitions and the different levels of coplanarity observed both in the S_0 and S_1 states. The 2,6-disubstituted dyes exhibited a significant bathochromic shift compared to their parent fluorophore scaffold (without carborane clusters) with a significant increase of the emission fluorescent quantum yields, owing to their higher level of coplanarity as assessed by theoretical calculations. On the other hand, the introduction of the two carborane units in 3,5-positions of the fluorophore led to a significant depletion of the fluorescence efficiency with regards to its homologous fluorophore. The scarce influence of solvent polarity observed on the absorption spectra of the new compounds, together with the absence of precipitation or aggregation phenomena, suggested high stability for all of them in organic solvents. The photophysical features observed in a water environment suggests a potential behavior of these dyes as fluorogenic probes, in which the fluorescence features might get restored upon binding or intercalation events with biological relevant molecules. Remarkably, the introduction of a short-terms oligoethylene glycol alkyl chain on the *meso*-phenyl ring had no effect on the PL properties of the dyes, allowing the design of pre- or post-functionalization strategies for the introduction of solubilizing groups on the fluorophore core.

This new family of dyes represent a promising structural extension to the well-established BODIPY set of fluorophores, widening the panorama of existing dyes absorbing in the therapeutical window. The most important PL properties (fluorescence efficiencies, Stokes shift, molar extinction coefficients, behavior in water) are in line with other common families of red-light emitting dyes [50]. Moreover, the introduction of two carborane units enhances the boron content of the dyes, improving the prospective applications of carborane-BODIPY dyes as potential boron carriers for BNCT applications. Taken together, these features make them promising candidates for further investigations in live-cell imaging and bio-supramolecular assays. Experiments aimed at evaluating both the internalization of the new dyes in several cell lines and the development of liposomal formulations are currently ongoing, and the results will be reported in due course.

CRediT authorship contribution statement

Chiara Bellomo: Investigation, Data curation, Formal analysis. **Davide Zanetti:** Investigation, Data curation, Formal analysis. **Francesca Cardano:** Investigation, Data curation, Formal analysis. **Sohini Sinha:** Investigation, Data curation, Formal analysis. **Mahdi Chaari:** Investigation, Data curation, Formal analysis. **Andrea Fin:** Validation, Data curation, Writing – review & editing, Supervision. **Andrea Maranzana:** Investigation, Data curation, Formal analysis, Writing – review & editing. **Rosario Núñez:** Conceptualization, Methodology,

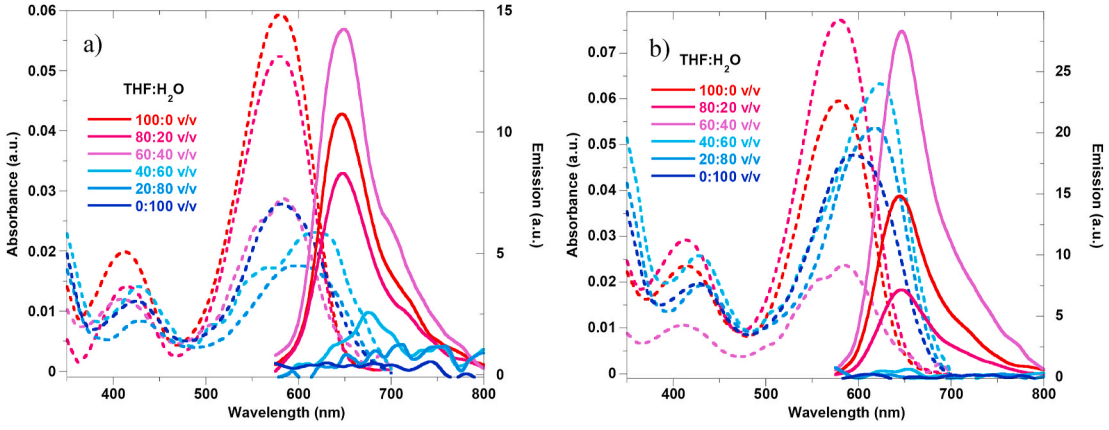

Fig. 7. UV–Vis absorption (dashed) and fluorescence (solid) spectra of BODIPY dyes (a) **3** and (b) **4** recorded in pure water and THF/water mixtures.

Validation, Data curation, Writing – original draft, Writing – review & editing, Supervision. **Marco Blangetti:** Conceptualization, Methodology, Validation, Data curation, Writing – original draft, Writing – review & editing, Supervision. **Cristina Prandi:** Conceptualization, Methodology, Validation, Writing – review & editing.

Declaration of competing interest

The authors declare that they have no known competing financial interests or personal relationships that could have appeared to influence the work reported in this paper.

Acknowledgements

We would like to acknowledge Dr. Emanuele Priola (UniTO) and Dr. Francesco Marra (UniTO) for technical support, and Prof. Claudio Medana (UniTO) for HRMS measurements. We acknowledge the italian MIUR, Huvepharma Italia srl, Regione Piemonte and Cassa di Risparmio di Torino for financial support. This research was funded by MINECO ((CTQ2016-75150-R) Agencia Estatal de Investigación AEI from MICINN (PID2019-106832RB-100/AEI/10.13039/501100011033) and Generalitat de Catalunya (2017 SGR1720). The work was also supported by the MICINN through the Severo Ochoa Program for Centers of Excellence FUNFUTURE (CEX2019-000917-S). Sohini Sinha was enrolled in the PhD Program of UAB. S. S. acknowledges financial support from DOC-FAM, European Union's Horizon 2020 research and innovation programme under the Marie Sklodowska-Curie grant agreement No 754397.

Appendix A. Supplementary data

Supplementary data to this article can be found online at https://doi.org/10.1016/j.dyepig.2021.109644.

References

[1] a) Grimes RN. Carboranes. third ed. US: Academic Press; 2016. p. 1058.b) Jelliss PA. In: Hosmane NS, editor. Boron Science: new Technologies and applications. Bosa Roca: Taylor & Francis; 2012. p. 355.
[2] a) Cabrera-Gonzalez J, Ferrer-Ugalde A, Bhattacharyya S, Chaari M, Teixidor F, Gierschner J, Núñez R. J Mater Chem C 2017;5:10211–9.b) Núñez R, Romero I, Teixidor F, Viñas C. Chem Soc Rev 2016;45:5147–73.
[3] a) Poater J, Viñas C, Bennour I, Escayola S, Solà M, Teixidor F. J Am Chem Soc 2020;142:9396–407.b) Poater J, Solà M, Viñas C, Teixidor F. Angew Chem Int Ed 2014;53:12191–5.
[4] Scholz M, Hey-Hawkins E. Chem Rev 2011;111:7035–62.
[5] Núñez R, Farràs P, Teixidor F, Viñas C, Sillanpää R, Kivekäs R. Angew Chem Int Ed 2006;45:1270–2.
[6] a) Leśnikowski ZJ. J Med Chem 2016;59:7738–58.b) Issa F, Kassiou M, Rendina LM. Chem Rev 2011;111:5701–22.c) Valliant JF, Guenther KJ, King AS, Morel P, Schaffer P, Sogbein OO, Stephenson KA. Coord Chem Rev 2002;232:173–230.
[7] a) Zhang X, Yan H. Coord Chem Rev 2019;378:466–82.b) Hey-Hawkins E, Viñas C. Boron-based compounds. Chichester, UK: John Wiley & Sons Ltd; 2018. p. 496.c) Duttwyler S. Pure Appl Chem 2018;90:733–44.d) Olid D, Núñez R, Viñas C, Teixidor F. Chem Soc Rev 2013;42:3318–36.e) Bregadze VI. Chem Rev 1992;92:209–23.
[8] a) Couto M, Alamón C, Nievas S, Perona M, Dagrosa MA, Teixidor F, Cabral P, Viñas C, Cerecetto H. Chem Eur J 2020;26:14335–40.b) Alamón C, Dávila B, García MF, Sánchez C, Kovacs M, Trias E, Barbeito L, Gabay M, Zeineh N, Gavish M, Teixidor F, Viñas C, Couto M, Cerecetto H. Cancers 2020;12:3423.c) Worm DJ, Hoppenz P, Els-Heindl S, Kellert M, Kuhnert R, Saretz S, Köbberling J, Riedl B, Hey-Hawkins E, Beck-Sickinger AG. J Med Chem 2020;63:2358–71.d) Viñas C, Núñez R, Bennour I, Teixidor F. Curr Med Chem 2019;26:5036–76.e) Buzharevski A, Paskas S, Sárosi M-B, Laube M, Lönnecke P, Neumann W, Mijatovic S, Maksimovic-Ivanic D, Pietzsch J, Hey-Hawkins E. ChemMedChem 2019;14:315–21.f) Calabrese G, Daou A, Rova A, Tseligka E, Vizirianakis IS, Fatouros DG, Tsibouklis J. MedChemComm 2017;8:67–72.g) Ban HS, Nakamura H. Chem Rec 2015;15:616–35.h) Soriano-Ursúa MA, Das BC, Trujillo-Ferrara JG. Expert Opin Ther Pat 2014;24:485–500.i) Viñas C. Future Med Chem 2013;5:617–9.
[9] Yinghuai Z, Hosmane NS. J Organomet Chem 2013;747:25–9.
[10] a) Schwartz JJ, Mendoza AM, Wattanatorn N, Zhao Y, Nguyen VT, Spokoyny AM, Mirkin CA, Baše T, Weiss PS. J Am Chem Soc 2016;138:5957–67.b) Wang J, Wang W-Y, Fang X-Y, Qiu Y-Q. J Mol Model 2015;21:1–10.c) Kaszynski P. In: Hosmane NS, editor. Boron Science: new Technologies and applications. Bosa Roca: Taylor & Francis; 2012. p. 319.
[11] a) Gan L, Chidambaram A, Fonquernie PG, Light ME, Choquesillo-Lazarte D, Huang H, Solano E, Fraile J, Viñas C, Teixidor F, Navarro JAR, Stylianou KC, Planas JG. J Am Chem Soc 2020;142:8299–311.b) Tan F, López-Periago A, Light ME, Cirera J, Ruiz E, Borrás A, Teixidor F, Viñas C, Domingo C, Planas JG. Adv Mater 2018;30:1800726.c) Saha A, Oleshkevich E, Viñas C, Teixidor F. Adv Mater 2017;29:1704238.d) Grzelczak MP, Danks SP, Klipp RC, Belic D, Zaulet A, Kunstmann-Olsen C, Bradley DF, Tsukuda T, Viñas C, Teixidor F, Abramson JJ, Brust M. ACS Nano 2017;11:12492–9.e) Qian EA, Wixtrom AI, Axtell JC, Saebi A, Jung D, Rehak P, Han Y, Moully EH, Mosallaei D, Chow S, Messina MS, Wang JY, Royappa AT, Rheingold AL, Maynard HD, Král P, Spokoyny AM. Nat Chem 2017;9:333–40.f) Sasaki T, Guerrero JM, Leonard AD, Tour JM. Nano Res 2008;1:412–9.g) Koshino M, Tanaka T, Solin N, Suenaga K, Isobe H, Nakamura E. Science 2007;316:853.
[12] a) Cabrera-González J, Chaari M, Teixidor F, Viñas C, Núñez R. Molecules 2020;25:1210.b) Chaari M, Kelemen Z, Choquesillo-Lazarte D, Teixidor F, Viñas C, Núñez R. Inorg Chem Front 2020;7:2370–80.c) Tao G, Duan Z, Mathey F. Org Lett 2019;21:2273–6.d) Chaari M, Cabrera-González J, Kelemen Z, Viñas C, Ferrer-Ugalde A, Choquesillo-Lazarte D, Ben Salah A, Teixidor F, Núñez R. J Organomet Chem 2018;865:206–13.e) Chaari M, Kelemen Z, Planas JG, Teixidor F, Choquesillo-Lazarte D, Ben Salah A, Viñas C, Núñez R. J Mater Chem C 2018;6:11336–47.f) Ferrer-Ugalde A, Cabrera-Gonzalez J, Juarez-Perez EJ, Teixidor F, Perez-Inestrosa E, Montenegro JM, Sillanpaa R, Haukka M, Núñez R. Dalton Trans 2017;46:2091–104.g) Cabrera-González J, Bhattacharyya S, Milián-Medina B, Teixidor F, Farfán N, Arcos-Ramos R, Vargas-Reyes V, Gierschner J, Núñez R. Eur J Inorg Chem 2017;2017:4575–80.h) Naito H, Nishino K, Morisaki Y, Tanaka K, Chujo Y. Angew Chem Int Ed 2017;56:254–9.i) Cabrera-González J, Viñas C, Haukka M, Bhattacharyya S, Gierschner J, Núñez R. Chem Eur J 2016;22:13588–98.j) Böhling L, Brockhinke A, Kahlert J, Weber L, Harder RA, Yufit DS, Howard JAK, MacBride JAH, Fox MA. Eur J Inorg Chem 2016;2016:403–12.k) Guo J, Liu D, Zhang J, Zhang J, Miao Q, Xie Z. Chem Commun 2015;51:12004–7.l) Ferrer-Ugalde A, Juarez-Perez EJ, Teixidor F, Viñas C, Sillanpaeae R, Perez-Inestrosa E, Núñez R. Chem Eur J 2012;18:544–53.
[13] a) Ochi J, Tanaka K, Chujo Y. Angew Chem Int Ed 2020;59:9841–55.b) Núñez R, Tarrés M, Ferrer-Ugalde A, de Biani FF, Teixidor F. Chem Rev 2016;116:14307–78.c) Mukherjee S, Thilagar P. Chem Commun 2016;52:1070–93.
[14] a) Ozdemir M, Choi D, Zorlu Y, Cosut B, Kim H, Kim C, Usta H. New J Chem 2017;41:6232–40.b) Ozcan E, Ozdemir M, Ho D, Zorlu Y, Ozdemir R, Kim C, Usta H, Cosut B. ChemPlusChem 2019;84:1423–31.
[15] Ho D, Ozdemir R, Kim H, Earmme T, Usta H, Kim C. ChemPlusChem 2019;84:18–37.
[16] a) Chaari M, Kelemen Z, Choquesillo-Lazarte D, Gaztelumendi N, Teixidor F, Viñas C, Nogués C, Núñez R. Biomater Sci 2019;7:5324–37.b) Nishino K, Yamamoto H, Ochi J, Tanaka K, Chujo Y. Chem Asian J 2019;14:1577–81.c) Tu D, Cai S, Fernandez C, Ma H, Wang X, Wang H, Ma C, Yan H, Lu C, An Z. Angew Chem Int Ed 2019;58:9129–33.d) Wu X, Guo J, Jia W, Zhao J, Jia D, Shan H. Dyes Pigments 2019;162:855–62.e) Li J, Yang C, Peng X, Chen Y, Qi Q, Luo X, Lai W-Y, Huang W. J Mater Chem C 2018;6:19–28.f) Nar I, Atsay A, Altındal A, Hamuryudan E. Inorg Chem 2018;57:2199–208.g) Li X, Tong X, Yin Y, Yan H, Lu C, Huang W, Zhao Q. Chem Sci 2017;8:5930–40.h) Wu A, Kolanowski JL, Boumelhem BB, Yang K, Lee R, Kaur A, Fraser ST, New EJ, Rendina LM. Chem Asian J 2017;12:1704–8.
[17] a) Loudet A, Burgess K. Chem Rev 2007;107:4891–932.b) Ulrich G, Ziessel R, Harriman A. Angew Chem Int Ed 2008;47:1184–201.
[18] a) Labra-Vázquez P, Flores-Cruz R, Galindo-Hernández A, Cabrera-González J, Guzmán-Cedillo C, Jiménez-Sánchez A, Lacroix PG, Santillan R, Farfán N, Núñez R. Chem Eur J 2020;26:16530–40.b) Nar I, Atsay A, Buyruk A, Pekbelgin Karaoglu H, Burat AK, Hamuryudan E. New J Chem 2019;43:4471–6.c) Wang H-Q, Ye J-T, Zhang Y, Zhao Y-Y, Qiu Y-Q. J Mater Chem C 2019;7:7531–47.d) Kim S-Y, Cho Y-J, Son H-J, Cho DW, Kang SO. J Phys Chem A 2018;122:3391–7.e) Berksun E, Nar I, Atsay A, Ozcesmeci I, Gelir A, Hamuryudan E. Inorg Chem Front 2018;5:200–7.f) Xuan S, Zhao N, Zhou Z, Fronczek FR, Vicente MGH. J Med Chem 2016;59:2109–17.g) Gibbs JH, Wang H, Bhupathiraju NVSDK, Fronczek FR, Smith KM, Vicente MGH. J Organomet Chem 2015;798:209–13.h) Jin GF, Cho Y-J, Wee K-R, Hong SA, Suh I-H, Son H-J, Lee J-D, Han W-S, Cho DW, Kang SO. Dalton Trans 2015;44:2780–7.i) Ziessel R, Ulrich G, Olivier JH, Bura T, Sutter A. Chem Commun 2010;46:7978–80.
[19] a) Lazzarato L, Gazzano E, Blangetti M, Fraix A, Sodano F, Picone GM, Fruttero R, Gasco A, Riganti C, Sortino S. Antioxidants 2019;8:531.b) Blangetti M, Fraix A, Lazzarato L, Marini E, Rolando B, Sodano F, Fruttero R, Gasco A, Sortino S. Chem Eur J 2017;23:9026–9.c) Parisotto S, Lace B, Artuso E, Lombardi C, Deagostino A, Scudu R, Garino C, Medana C, Prandi C. Org Biomol Chem 2017;15:884–93.d) Fraix A, Blangetti M, Guglielmo S, Lazzarato L, Marino N, Cardile V, Graziano ACE, Manet I, Fruttero R, Gasco A, Sortino S. Chem Med Chem 2016;11:1371–9.e) Prandi C, Ghigo G, Occhiato EG, Scarpi D, Begliomini S, Lace B, Alberto G, Artuso E, Blangetti M. Org Biomol Chem 2014;12:2960–8.f) Prandi C, Rosso H, Lace B, Occhiato EG, Oppedisano A, Tabasso S, Alberto G, Blangetti M. Mol Plant 2013;6:113–27.
[20] Bellomo C, Chaari M, Cabrera-Gonzalez J, Blangetti M, Lombardi C, Deagostino A, Viñas C, Gaztelumendi N, Nogués C, Núñez R, Prandi C. Chem Eur J 2018;24:15622–30.
[21] Guo Z, Park S, Yoon J, Shin I. Chem Soc Rev 2014;43:16–29.
[22] Boens N, Verbelen B, Dehaen W. Eur J Org Chem 2015;2015:6577–95.
[23] Gai L, Mack J, Lu H, Yamada H, Kuzuhara D, Lai G, Li Z, Shen Z. Chem Eur J 2014;20:1091–102.

[24] Wu Y, Ma X, Jiao J, Cheng Y, Zhu C. Synlett 2012;23:778–82.
[25] Yang P, Zhao J, Wu W, Yu X, Liu Y. J Org Chem 2012;77:6166–78.
[26] Volkova YA, Brizet B, Harvey PD, Averin AD, Goze C, Denat F. Eur J Org Chem 2013;2013:4270–9.
[27] Brouwer AM. Pure Appl Chem 2011;83:2213–28.
[28] Yanai T, Tew DP, Handy NC. Chem Phys Lett 2004;393:51–7.
[29] a) Ditchfield R, Hehre WJ, Pople JA. J Chem Phys 1971;54:724–8.b) Hehre WJ, Ditchfield R, Pople JA. J Chem Phys 1972;56:2257–61.
[30] Marenich AV, Cramer CJ, Truhlar DG. J Phys Chem B 2009;113:6378–96.
[31] Tomasi J, Mennucci B, Cancès E. J Mol Struc Theochem 1999;464:211–26.
[32] Cammi R, Mennucci B, Tomasi J. J Phys Chem A 2000;104:5631–7.
[33] Cohen AJ, Handy NC. Mol Phys 2001;99:607–15.
[34] Gaussian 16, Revision B0.1, Frisch MJ, Trucks GW, Schlegel HB, Scuseria GE, Robb MA, Cheeseman JR, Scalmani G, Barone V, Petersson GA, Nakatsuji H, Li X, Caricato M, Marenich A, Bloino J, Janesko BG, Gomperts R, Mennucci B, Hratchian HP, Ortiz JV, Izmaylov AF, Sonnenberg JL, Williams-Young D, Ding F, Lipparini F, Egidi F, Goings J, Peng B, Petrone A, Henderson T, Ranasinghe D, Zakrzewski VG, Gao J, Rega N, Zheng G, Liang W, Hada M, Ehara M, Toyota K, Fukuda R, Hasegawa J, Ishida M, Nakajima T, Honda Y, Kitao O, Nakai H, Vreven T, Throssell K, Montgomery Jr JA, Peralta JE, Ogliaro F, Bearpark M, Heyd JJ, Brothers E, Kudin KN, Staroverov VN, Keith T, Kobayashi R, Normand J, Raghavachari K, Rendell A, Burant JC, Iyengar SS, Tomasi J, Cossi M, Millam JM, Klene M, Adamo C, Cammi R, Ochterski JW, Martin RL, Morokuma K, Farkas O, Foresman JB, Fox DJ. Wallingford CT: Gaussian, Inc.; 2016.
[35] GaussView Version 6, Dennington Roy, Keith Todd A, Millam John M. Shawnee Mission, KS: Semichem Inc.; 2016.
[36] Rohand T, Qin W, Boens N, Dehaen W. Eur J Org Chem 2006;2006:4658–63.
[37] Gibbs JH, Robins LT, Zhou Z, Bobadova-Parvanova P, Cottam M, McCandless GT, Fronczek FR, Vicente MGH. Bioorg Med Chem 2013;21:5770–81.
[38] Gorbe M, Costero AM, Sancenón F, Martínez-Máñez R, Ballesteros-Cillero R, Ochando LE, Chulvi K, Gotor R, Gil S. Dyes Pigments 2019;160:198–207.
[39] Littke AF, Fu GC. J Am Chem Soc 2001;123:6989–7000.
[40] Fristrup P, Le Quement S, Tanner D, Norrby P. Organometallics 2004;23:6160–5.
[41] Shirasaki Y. The introduction of nonionic amphiphile chains enhance aqueous solubility without a large loss of lipophilicity. J Pharmacol Sci 2008;97:2462–96. See for details.
[42] Leushina EA, Usol'tsev IA, Bezzubov SI, Moiseeva AA, Terenina MV, Anisimov AV, Taydakov IV, Khoroshutin AV. Dalton Trans 2017;46:17093–100.
[43] Rurack K, Kollmannsberger M, Daub J. New J Chem 2001;25:289–92.
[44] Hu W, Lin Y, Zhang X-F, Feng M, Zhao S, Zhang J. Dyes Pigments 2019;164:139–47.
[45] Ziessel R, Ulrich G, Harriman A. New J Chem 2007;31:496–501.
[46] a) Chen Y, Zhao J, Guo H, Xie L. J Org Chem 2012;77:2192–206.b) Kee HL, Kirmaier C, Yu L, Thamyongkit P, Youngblood WJ, Calder ME, Ramos L, Noll BC, Bocian DF, Scheidt WR, Birge RR, Lindsey JS, Holten D. J Phys Chem B 2005;109:20433–43.
[47] Grabowski ZR, Rotkiewicz K, Rettig W. Chem Rev 2003;103:3899–4032.
[48] Liptay W. Angew Chem Int Ed 1969;8:177–88.
[49] Filarowski A, Kluba M, Cieślik-Boczula K, Koll A, Kochel A, Pandey L, De Borggraeve WM, Van der Auweraer M, Catalán J, Boens N. Photochem Photobiol Sci 2010;9:996–1008.
[50] a) Escobedo JO, Rusin O, Lim S, Strongin RM. Curr Opin Chem Biol 2010;14:64–70.b) Rurack K, Spieles M. Anal Chem 2011;83:1232–42.